University of Zurich[UZH] | ETH Eidgenössische Technische Hochschule Zürich Swiss Federal Institute of Technology Zurich

KING'S College LONDON

Beyond Nyquist – Accelerating Magnetic Resonance Imaging

Sebastian Kozerke
Institute for Biomedical Engineering, University and ETH Zurich, Switzerland
Imaging Sciences and Biomedical Engineering, King's College London, UK

It’s useful…

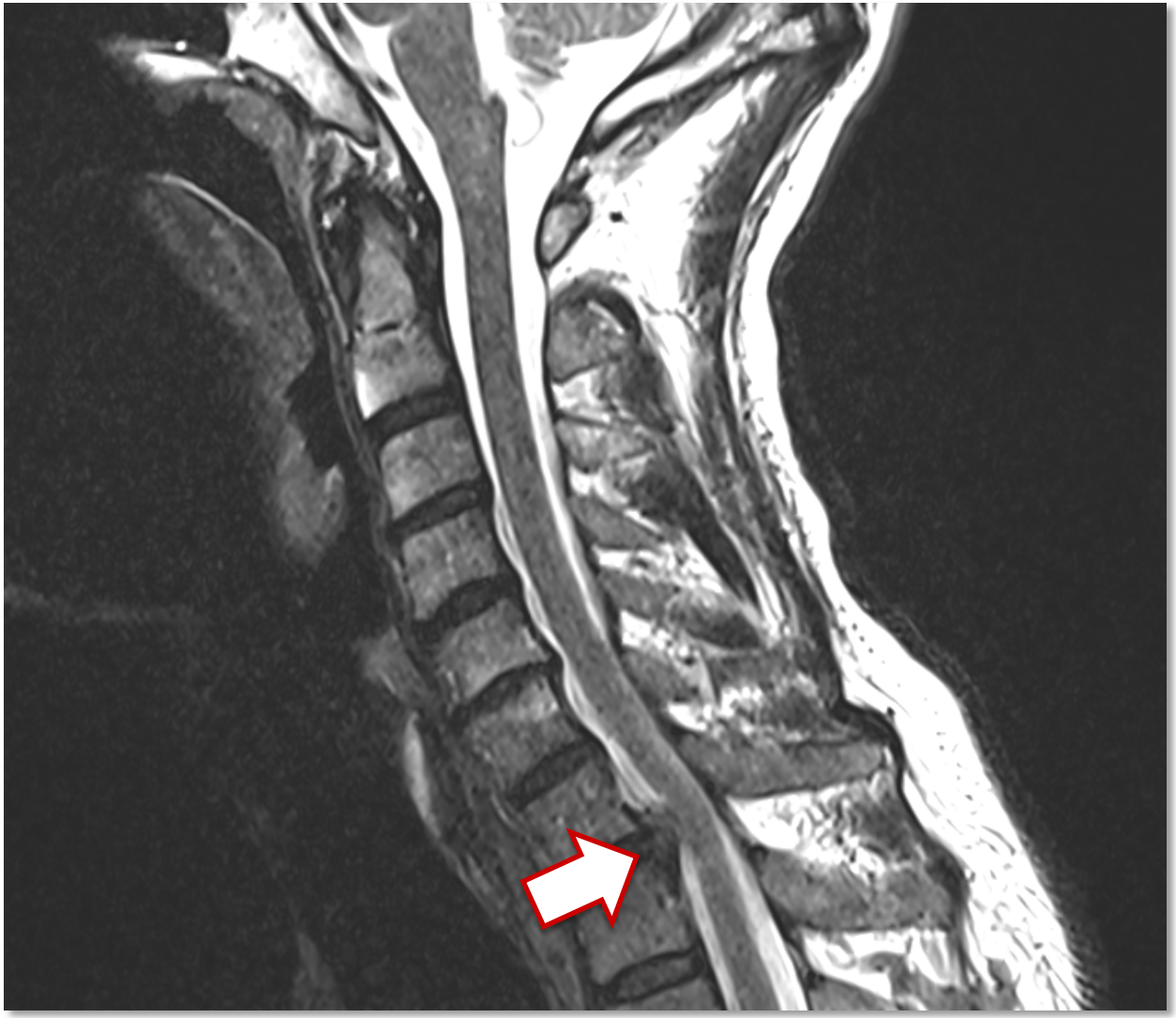

Blood flow quantification

Healthy volunteer

Patient with dilated aorta

7D encoding (x-y-z-v_x-v_y-v_z-t)
2x2x2 mm^3

Magnetic Resonance Imaging

Radio transmitter

Position ➔ Frequency

Signal source

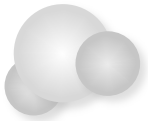

Radio receiver

Magnetic field

Frequency ➔ Position

Encoding

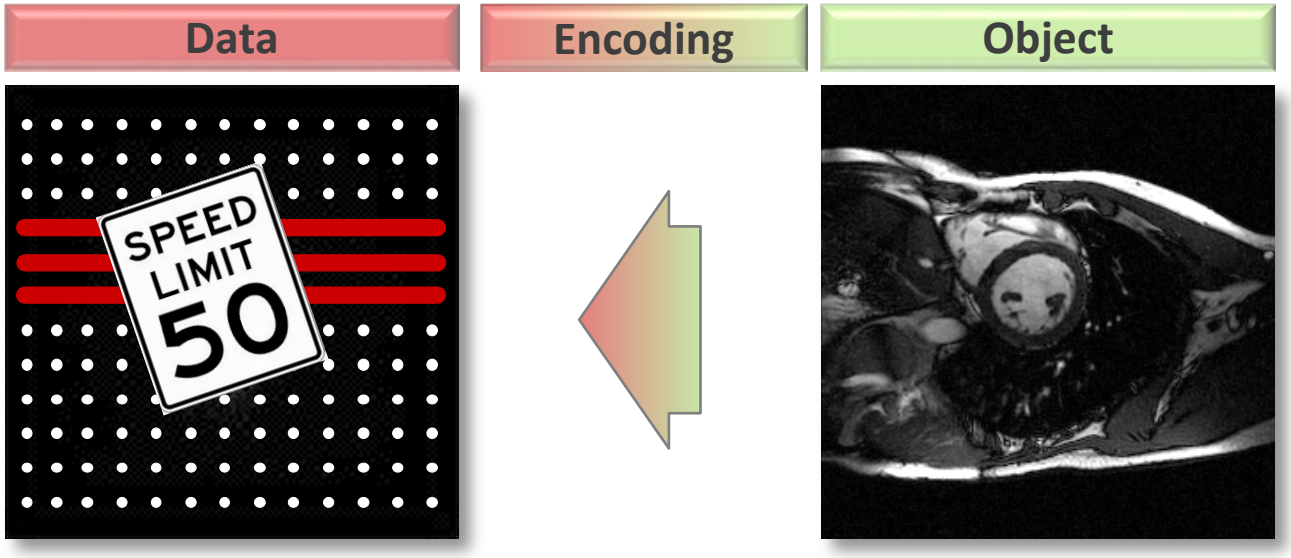

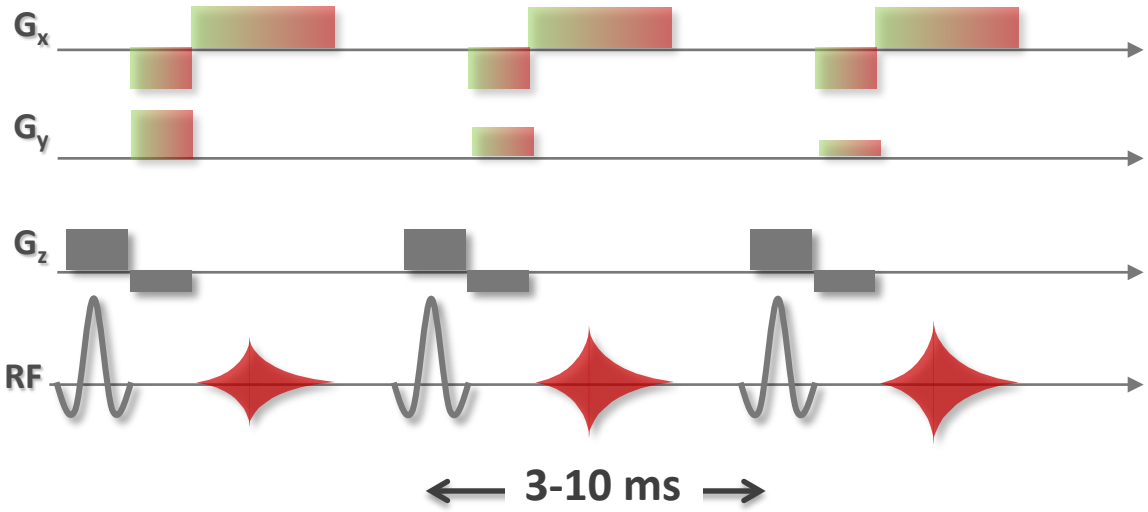

Encoding

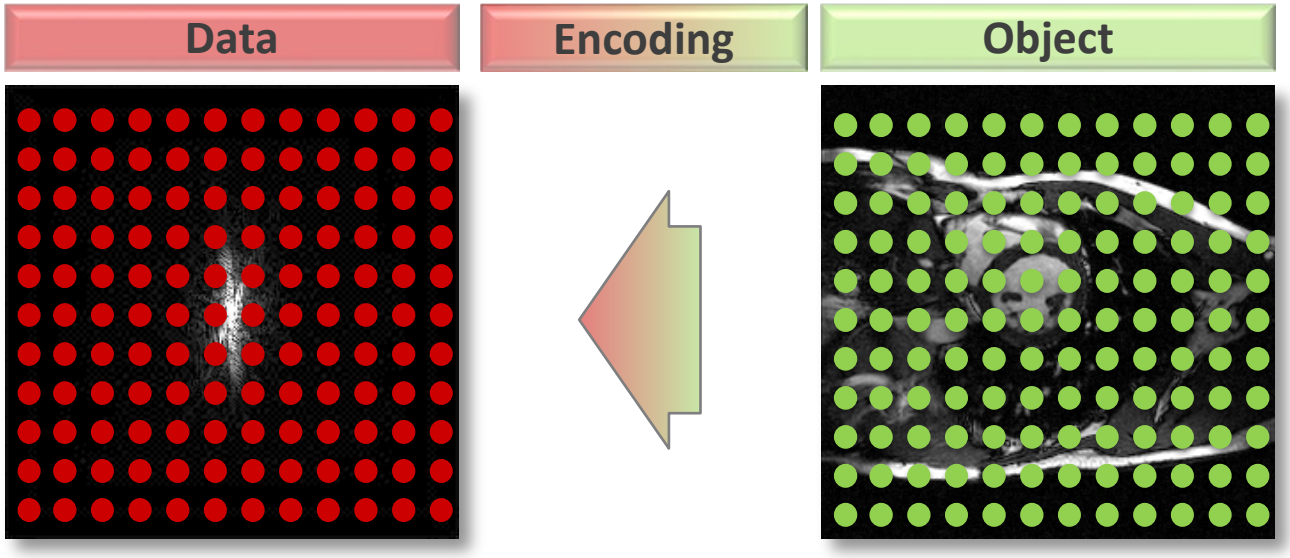

$$d_\kappa = \int e^{j\vec{k}_\kappa \cdot \vec{x}} \rho(\vec{x}) d\vec{x}$$

$$d_\kappa = \sum_\xi e^{j\vec{k}_\kappa \cdot \vec{x}_\xi} \rho(\vec{x}_\xi)$$

$$\vec{d} = E \vec{\rho}$$

Decoding

Data

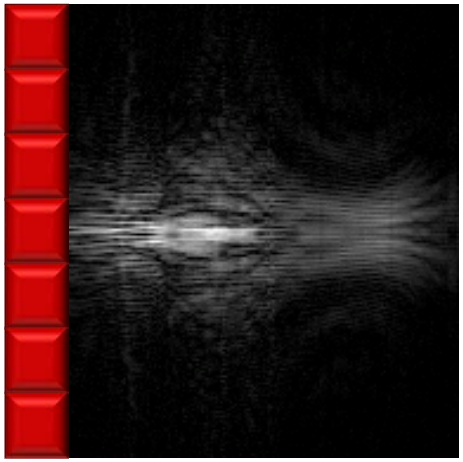

?

Image

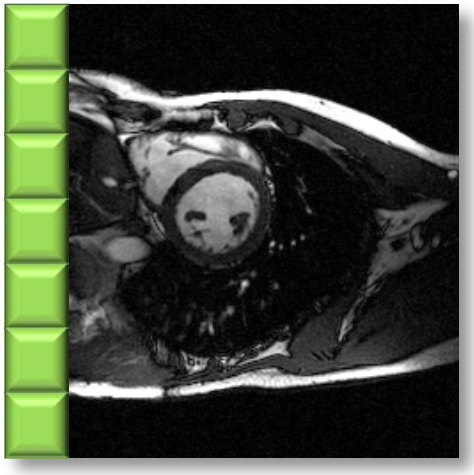

Encoding

$$\vec{d} = E \cdot \vec{\rho} + \vec{\eta}$$

Decoding

$$\vec{i} = \left(E^H \Psi^{-1} E\right)^{-1} E^H \Psi^{-1} \cdot \vec{d}$$

$$\vec{i} \rightarrow \operatorname{argmin}_i \left(\vec{d} - E \cdot \vec{i}\right)^H \Psi^{-1} \left(\vec{d} - E \cdot \vec{i}\right)$$

Linear decoding

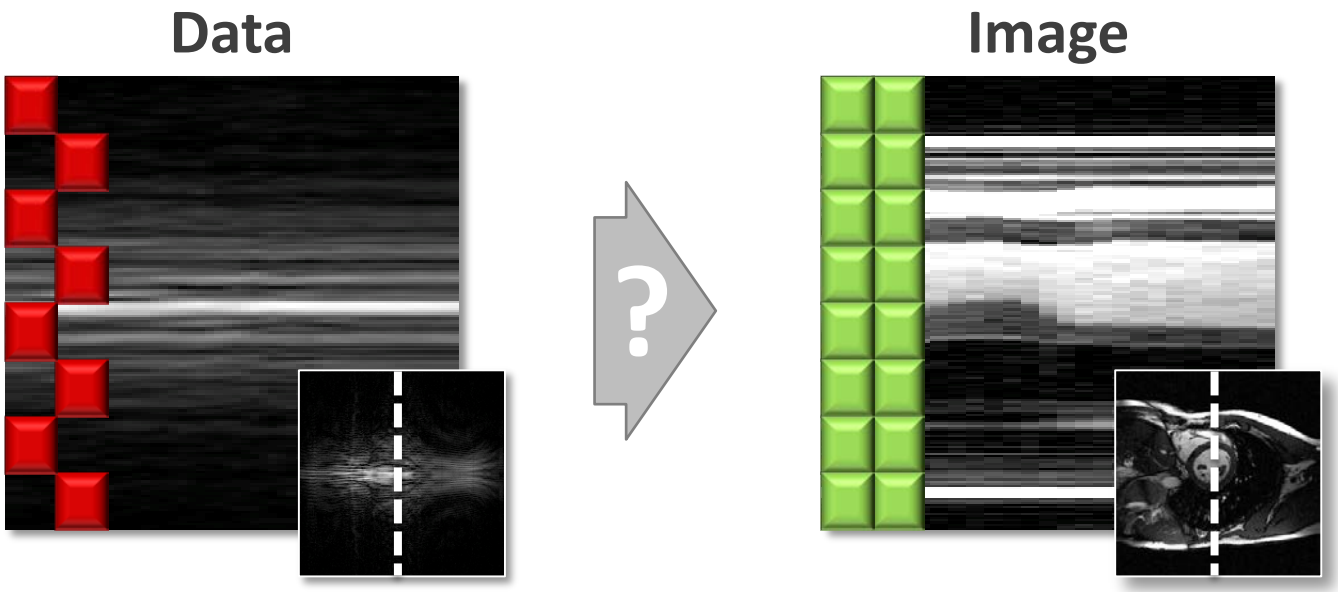

$$\vec{i} \rightarrow \quad \operatorname{argmin}_i \left\| \vec{d} - E \cdot \vec{i} \right\|_2^2$$

$$\vec{i} \rightarrow \quad \operatorname{argmin}_i \left\| \vec{d} - E \cdot \vec{i} \right\|_2^2 + \lambda \left\| \Theta^{-1} \cdot i \right\|_2$$

Prior info

Transform coding

x-t space

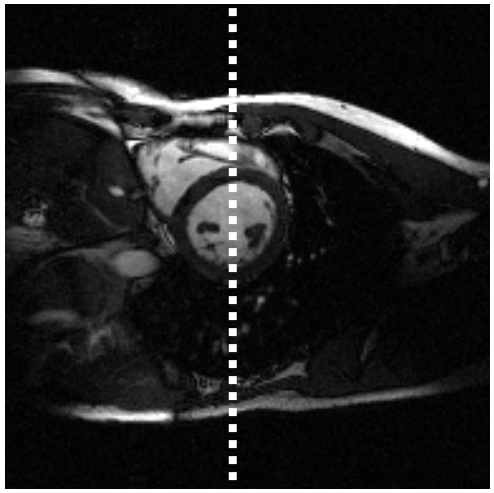

x-t space

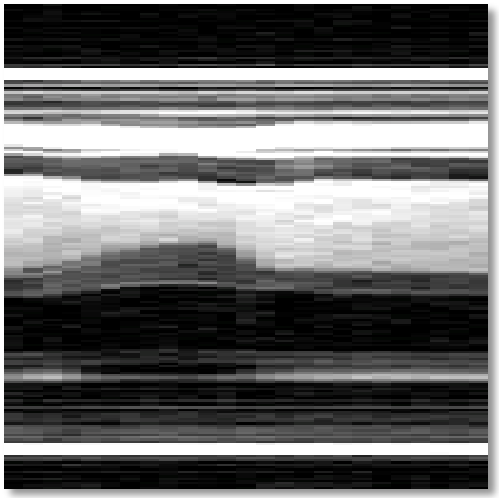

x-f space

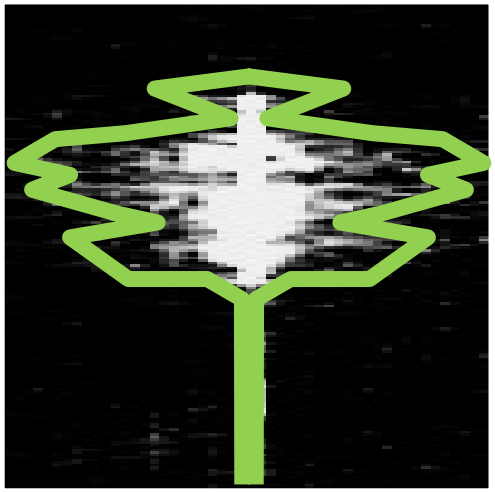

$$\tilde{\rho}\left(x, f_{\varphi}\right) = \sum e^{j2\pi f_{\varphi} t_{\tau}} \rho\left(x, t_{\tau}\right)$$

Madore B et al. MRM 1999 Tsao J et al. MRM 2002

Transform coding

Harry Nyquist
1889-1976

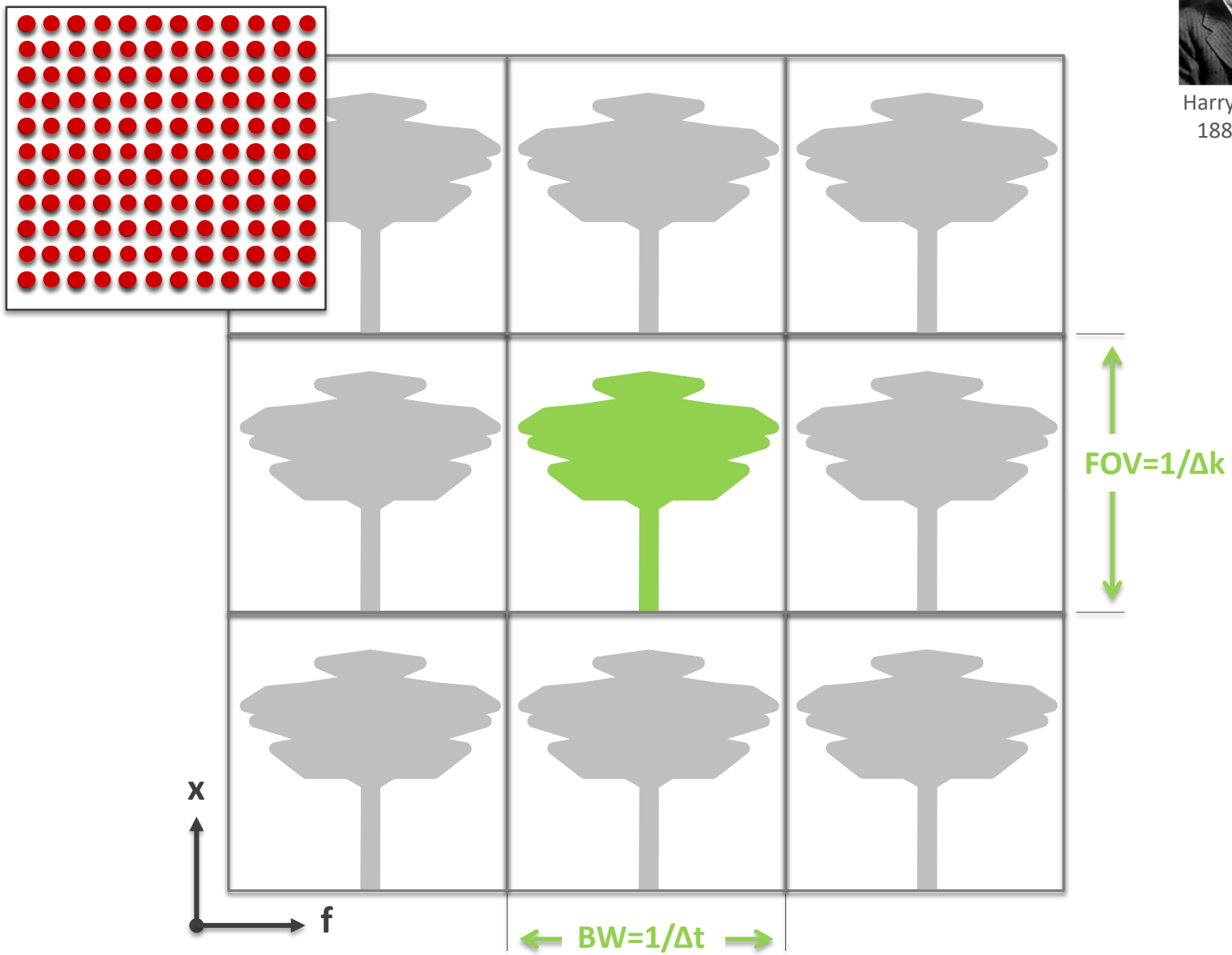

Transform coding

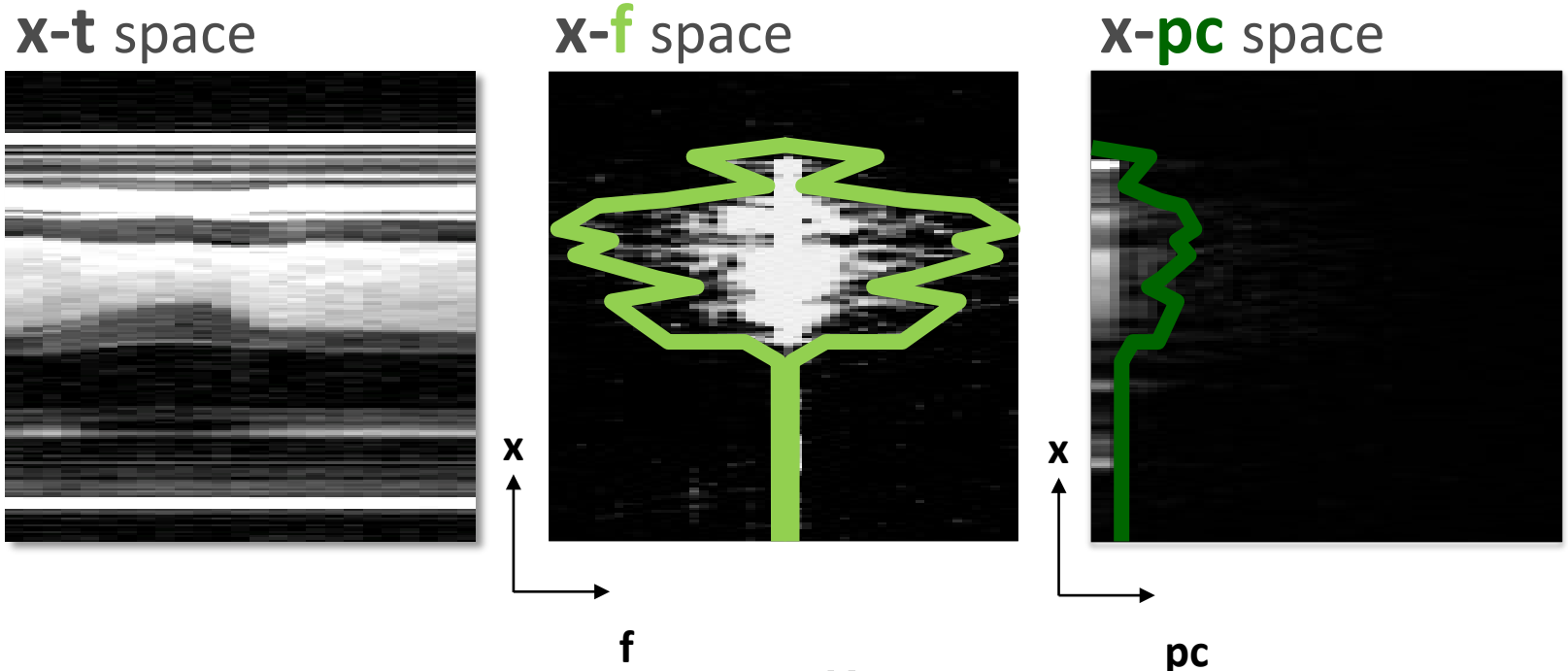

$$\tilde{\rho}(x,f) = UEV^H = \sum_{n=1}^{pc} w(x,n)\, b(n,f)$$

Pedersen H et al. MRM 2009

Linear decoding

Temporal regularization

$$\vec{i} \rightarrow \operatorname{argmin}_i \left\| \vec{d} - E \cdot \vec{i} \right\|_2^2 + \lambda \left\| \Phi_t \vec{i} \right\|_2^2$$

Spatiotemporal regularization

$$\vec{i} \rightarrow \operatorname{argmin}_i \left\| \vec{d} - E \cdot \vec{i} \right\|_2^2 + \lambda \left\| \Phi_{x,t} \vec{i} \right\|_2^2$$

Spatiotemporal training ($R < N_c$)

$$\vec{w} = \left(\tilde{E}^H \tilde{\Psi}^{-1} \tilde{E} + \lambda \tilde{\Theta}^{-1} \right)^{-1} \tilde{E}^H \tilde{\Psi}^{-1} \vec{d}$$

Spatiotemporal training ($R > N_c$)

$$\vec{w} = \tilde{\Theta} \tilde{E}^H \left(\tilde{E} \tilde{\Theta} \tilde{E}^H + \lambda \tilde{\Psi} \right)^{-1} \vec{d}$$

k-t PCA

Tsao J et al. MRM 2003 Kozerke S et al. MRM 2004 Pedersen H et al. MRM 2009

k-t PCA

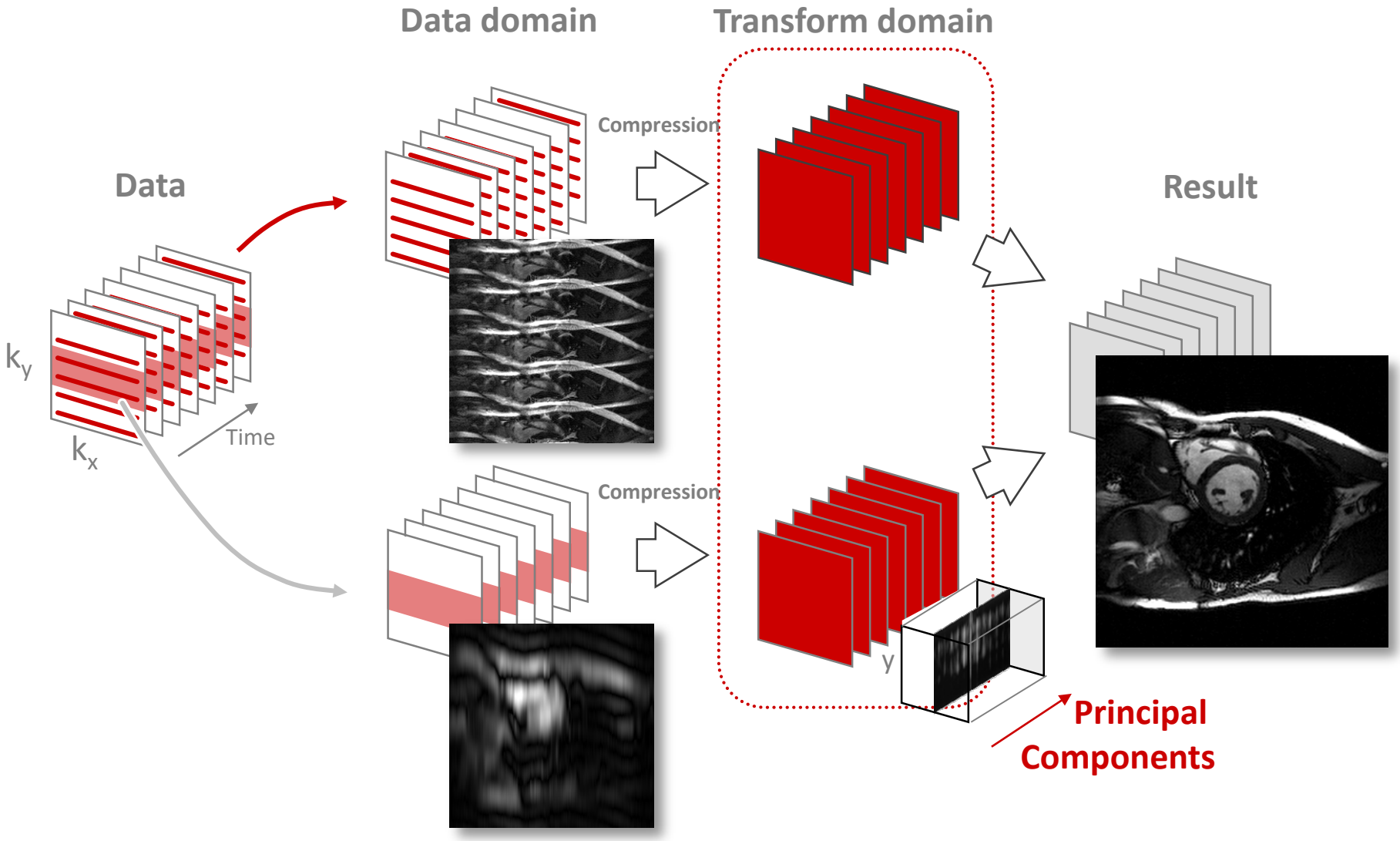

Pedersen H et al. MRM 2009 Vitanis V et al. IEEE 2010 Giese D et al. MRM 2013 Knobloch V et al. MRM 2013

Nonlinear decoding

Temporal regularization

$$\vec{i} \rightarrow \operatorname{argmin}_i \left\| \vec{d} - E \cdot \vec{i} \right\|_2^2 + \lambda \left\| \Phi_t \vec{i} \right\|_2^2$$

Spatiotemporal regularization

$$\vec{i} \rightarrow \operatorname{argmin}_i \left\| \vec{d} - E \cdot \vec{i} \right\|_2^2 + \lambda \left\| \Phi_{x,t} \vec{i} \right\|_2^2$$

Compressed Sensing

$$\vec{i} \rightarrow \operatorname{argmin}_i \left\| \vec{d} - E \cdot \vec{i} \right\|_2^2 + \lambda \left\| \Phi_{x,f} \vec{i} \right\|_1$$

Low-rank sparse decomposition

$$\vec{i} \rightarrow \operatorname{argmin}_i \left\| \vec{d} - E \cdot (L + S) \right\|_2^2 + \lambda_L \left\| L \right\|_* + \lambda \left\| S \right\|_1$$

Lustig M et al. MRM 2007 Gamper U et al. MRM 2008 Otazo R et al. ISMRM 2013

Compressed Sensing

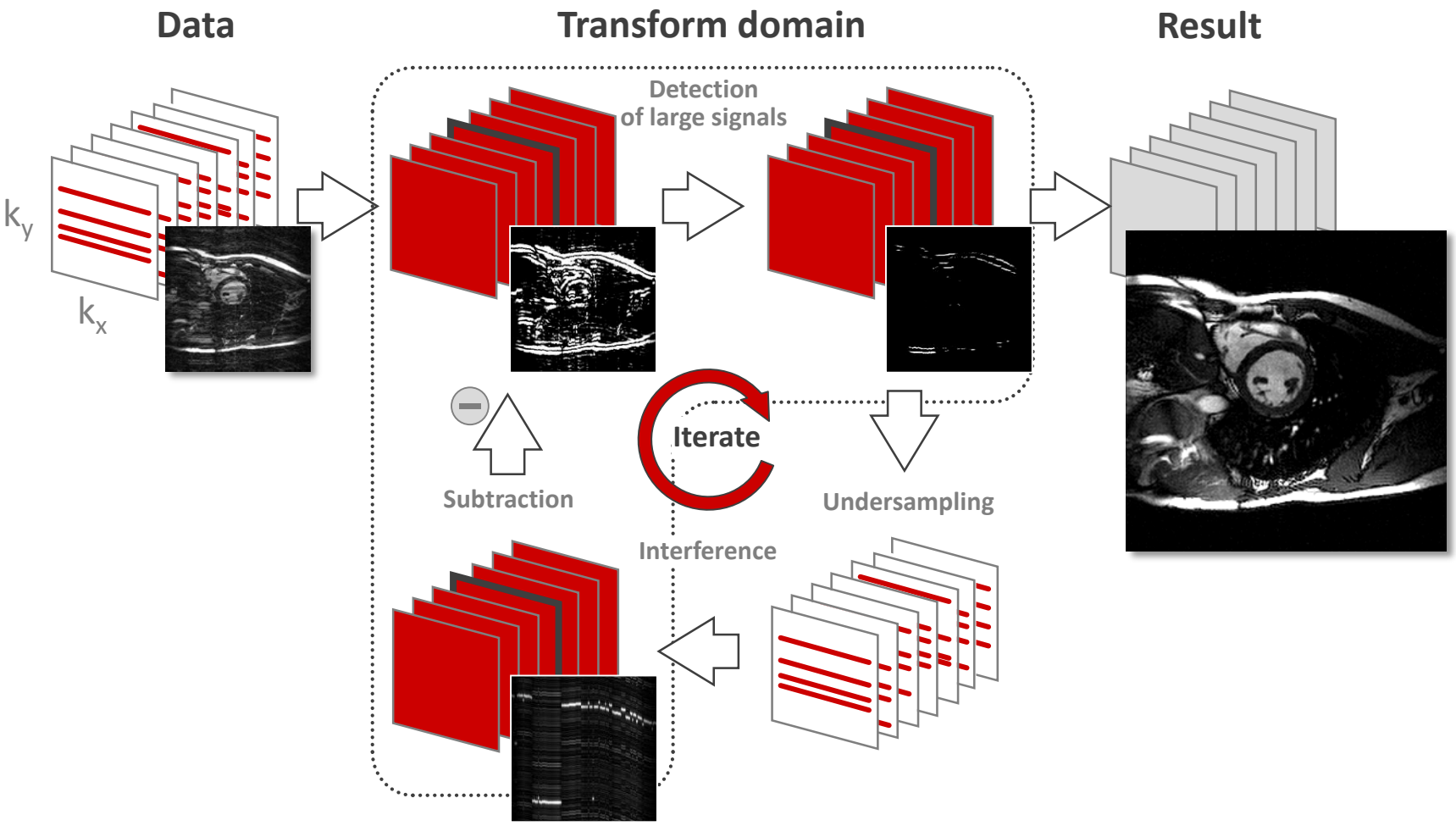

Undersampling progress – Cardiac

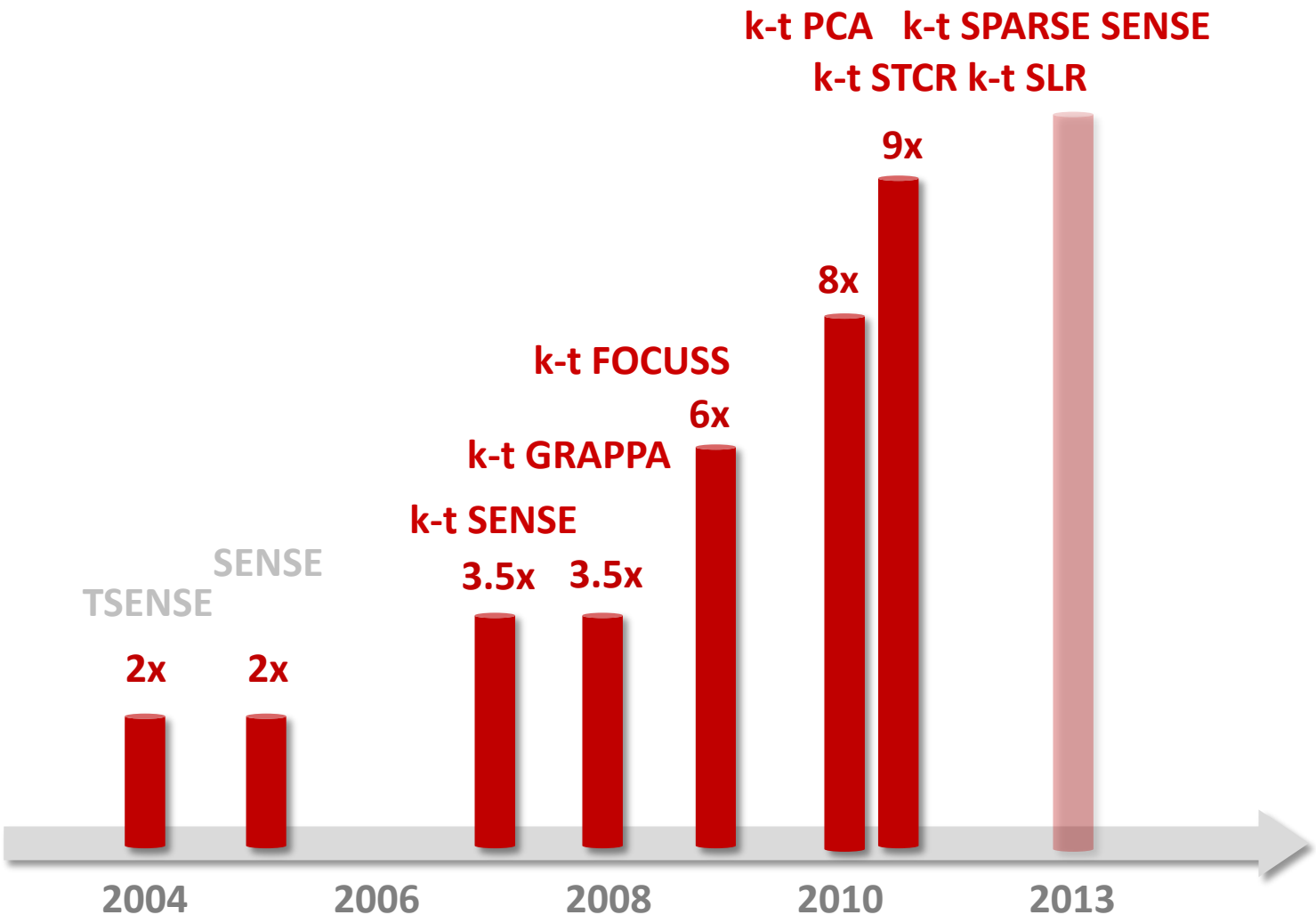

Kellman P et al. MRM 2004
Plein S et al. Radiology 2005
Plein S et al. MRM 2007
Jung B et al. JMRI 2008
Nayak KS et al. JCMR 2008
Vitanis V et al. MRM 2010
Otazo R et al. MRM 2010
Lingala SG et al. IEEE 2011

Blood flow quantification

Healthy volunteer

Patient with dilated aorta

Reconstruction accuracy

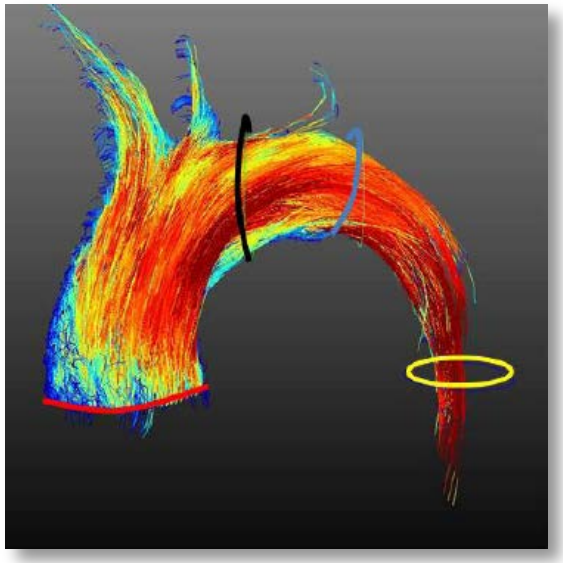

R=1 R=4 R=8 R=16

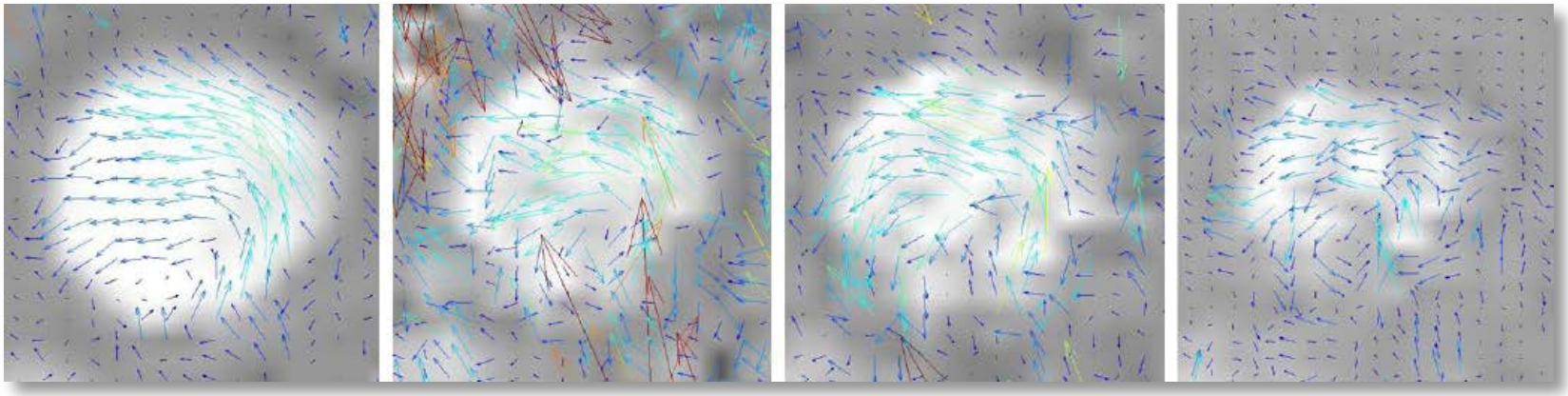

J. Busch et al. MRM 2013

Divergence-free image reconstruction

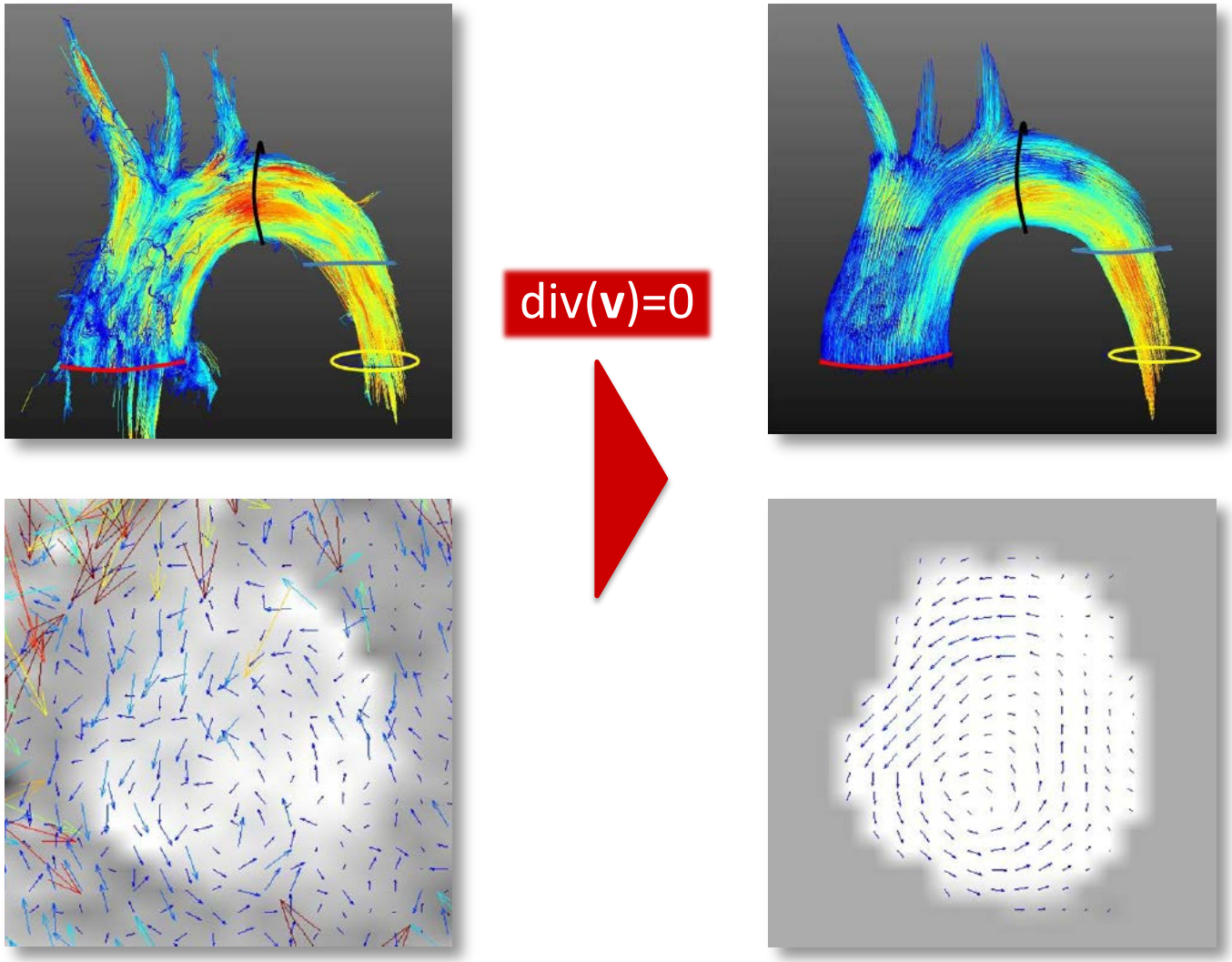

J. Busch et al. MRM 2013

Divergence-free image reconstruction

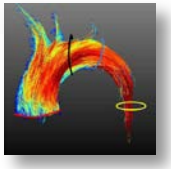

R=1 R=4 R=8

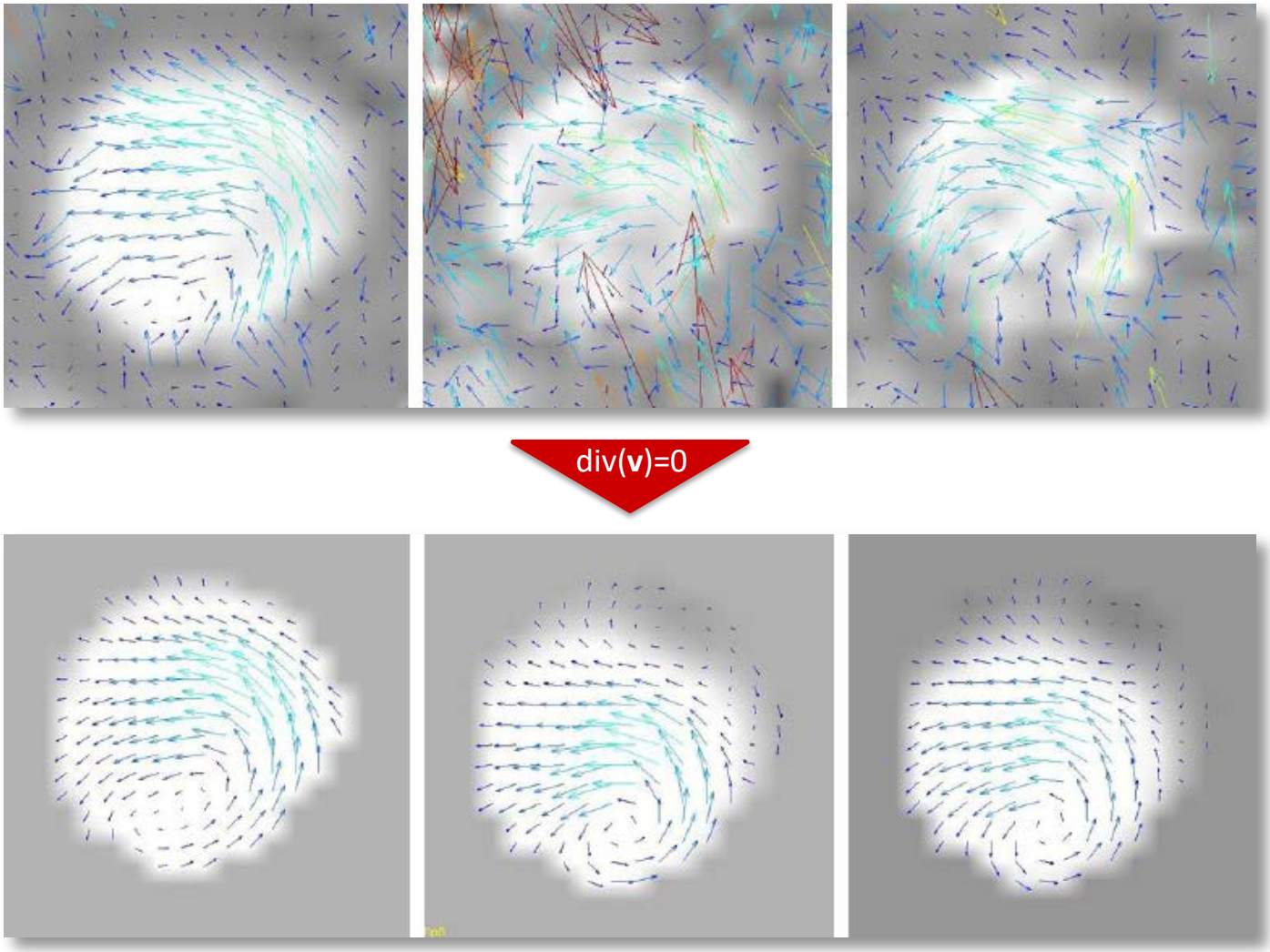

J. Busch et al. MRM 2013

Image reconstruction in non-linear feature spaces

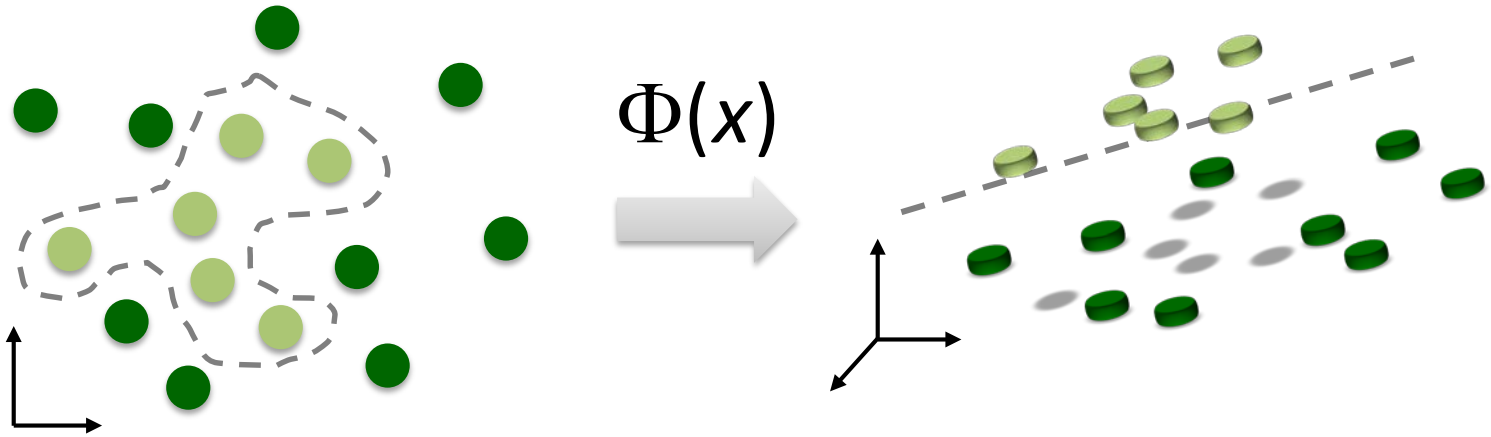

$$\vec{i} \rightarrow \qquad \vec{i}_{n+1} = \mathcal{P}_{kPCA}\left(\vec{i}_n - E^H\left(E\vec{i}_n - \vec{d}\right)\right)$$

Schmidt J et al. PLOS ONE 2016

Image reconstruction in non-linear feature spaces

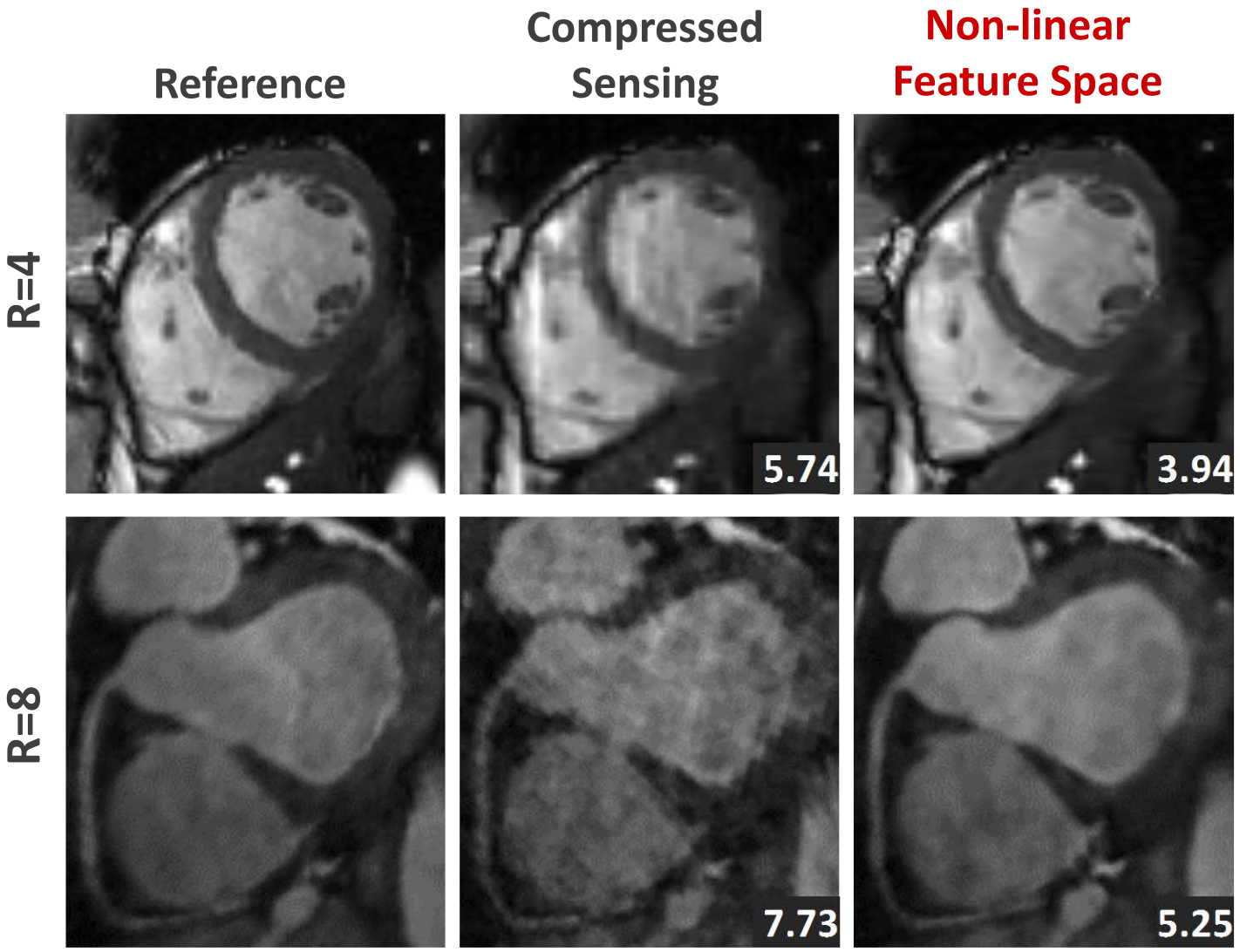

Schmidt J et al. PLOS ONE 2016

Ischemic cascade

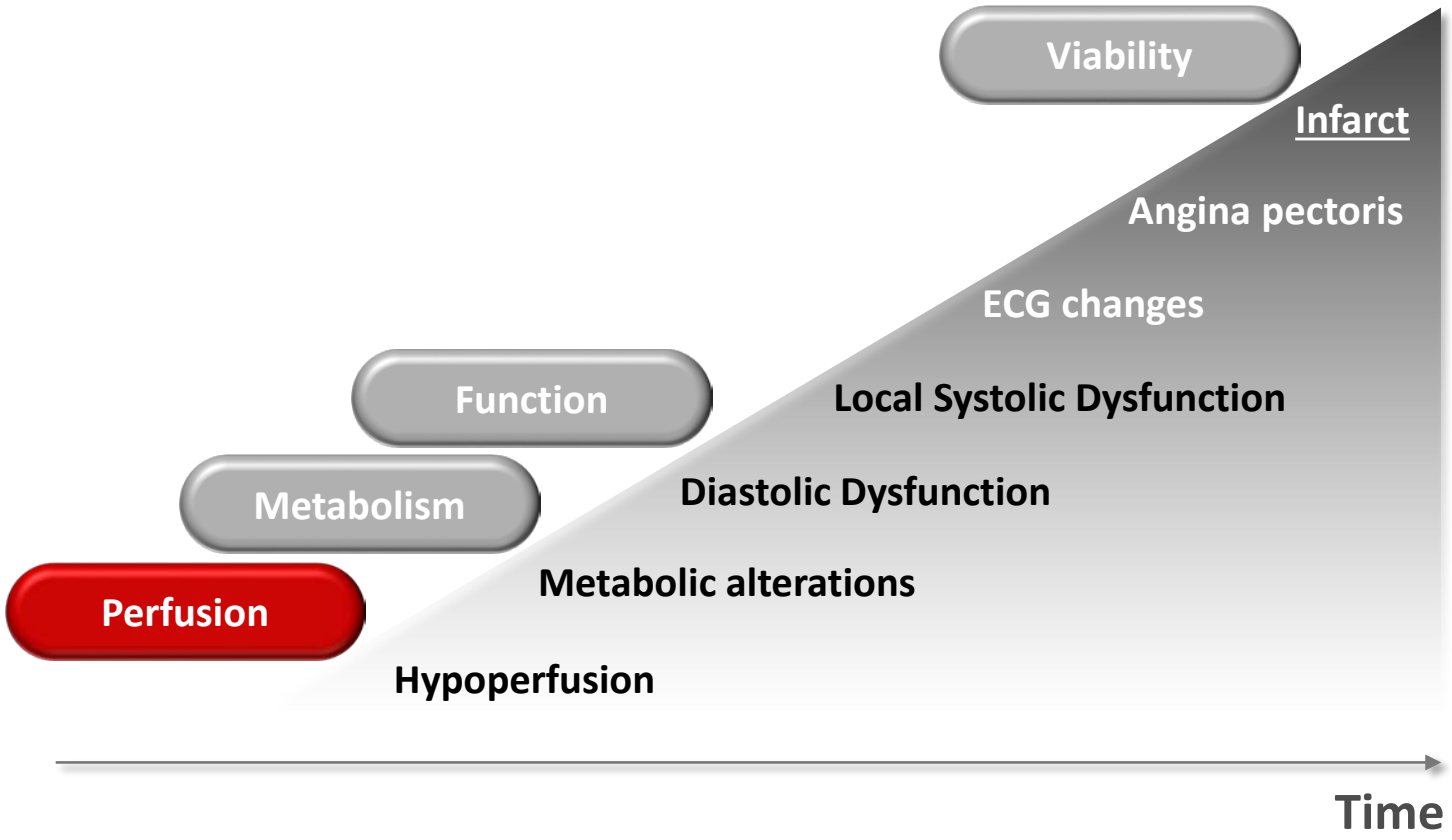

3D dynamic perfusion imaging

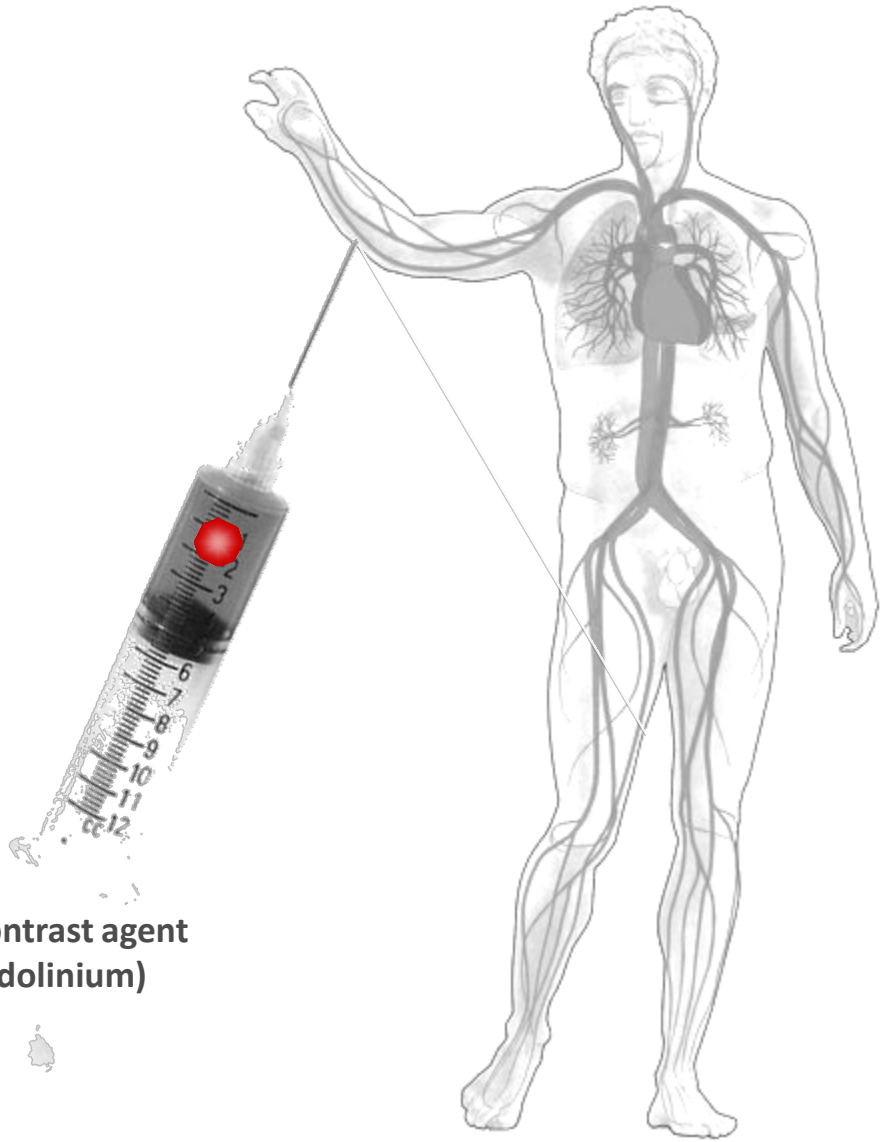

2D Perfusion imaging

5x 2D k-t SENSE (1.1 x 1.1 mm^2)

Stress PET

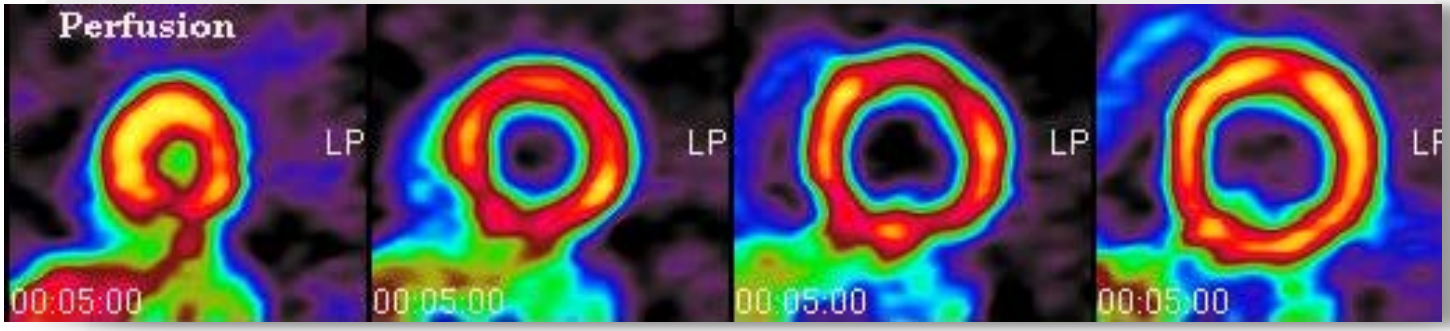

Plein S et al. MRM 2008, Radiology 2009

k-t PCA

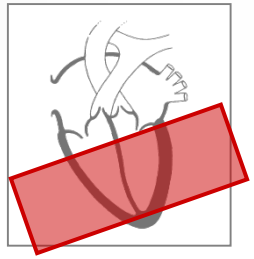

10x k-t PCA (2.2x2.2x10 mm^3)

Vitanis V et al. MRM 2011, Manka R et al. JACC 2011, Jogyia R et al. JACC 2012

3D Perfusion trial

3D Perfusion Multi-centre study

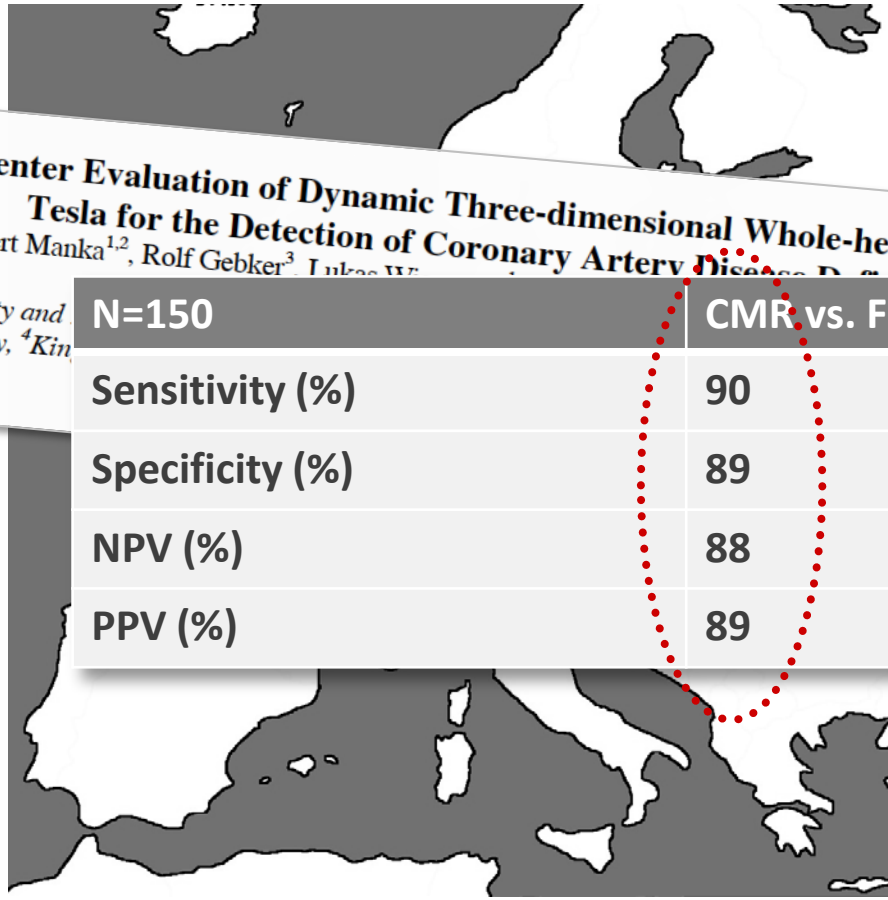

Multicenter Evaluation of Dynamic Three-dimensional Whole-heart Myocardial Perfusion Imaging at 3.0 Tesla for the Detection of Coronary Artery Disease

Robert Manka[1,2], Rolf Gebker[3], Lukas W...

[1]University and ... Germany, [4]Kin...

...serve

...tz[6], Bernhard

...te Berlin, Berlin, ...Hospital RWTH

N=150	CMR vs. FFR	CMR vs. QCA
Sensitivity (%)	90	77
Specificity (%)	89	94
NPV (%)	88	68
PPV (%)	89	96

Manka R et al. Circ CVI 2015

Motion artifacts

10x 3D k-t PCA (2.2 x 2.2 mm^2)

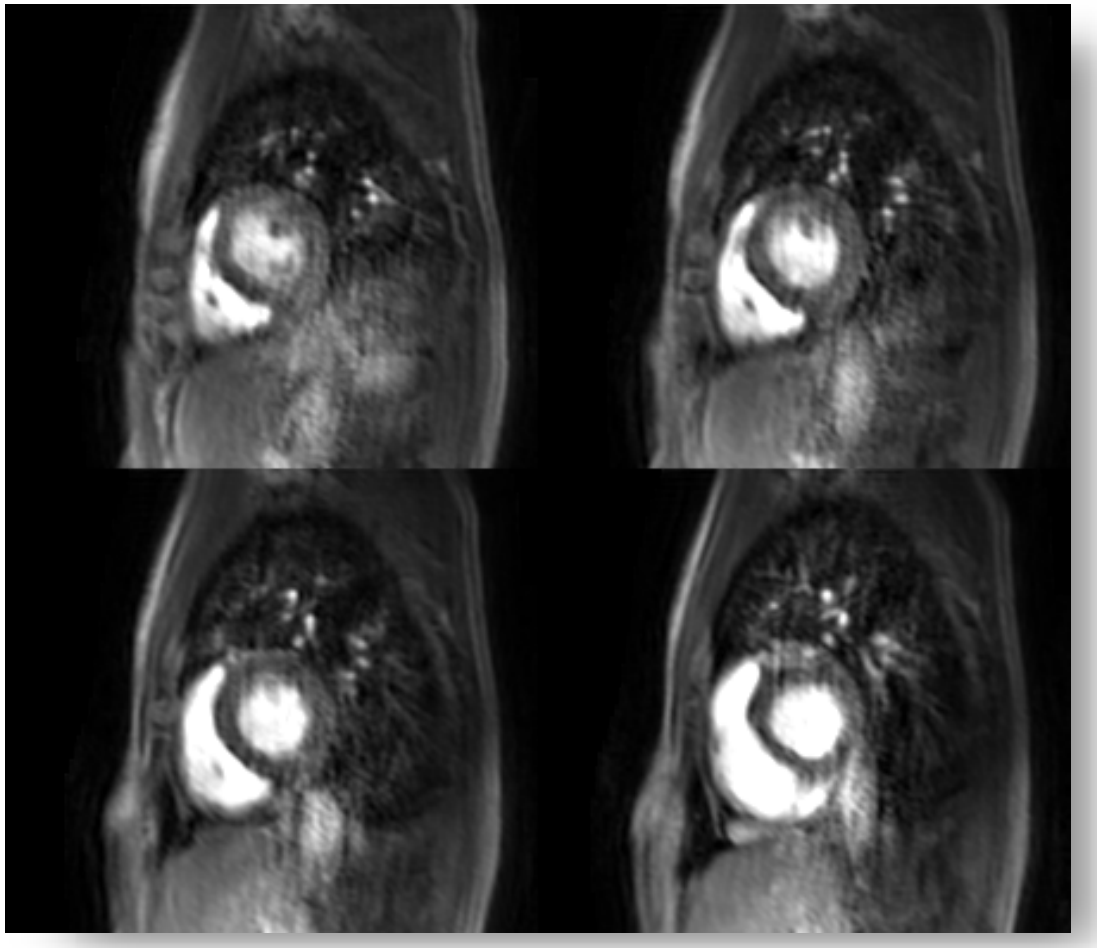

Schmidt JF et al. MRM 2013

Generic matrix description of motion

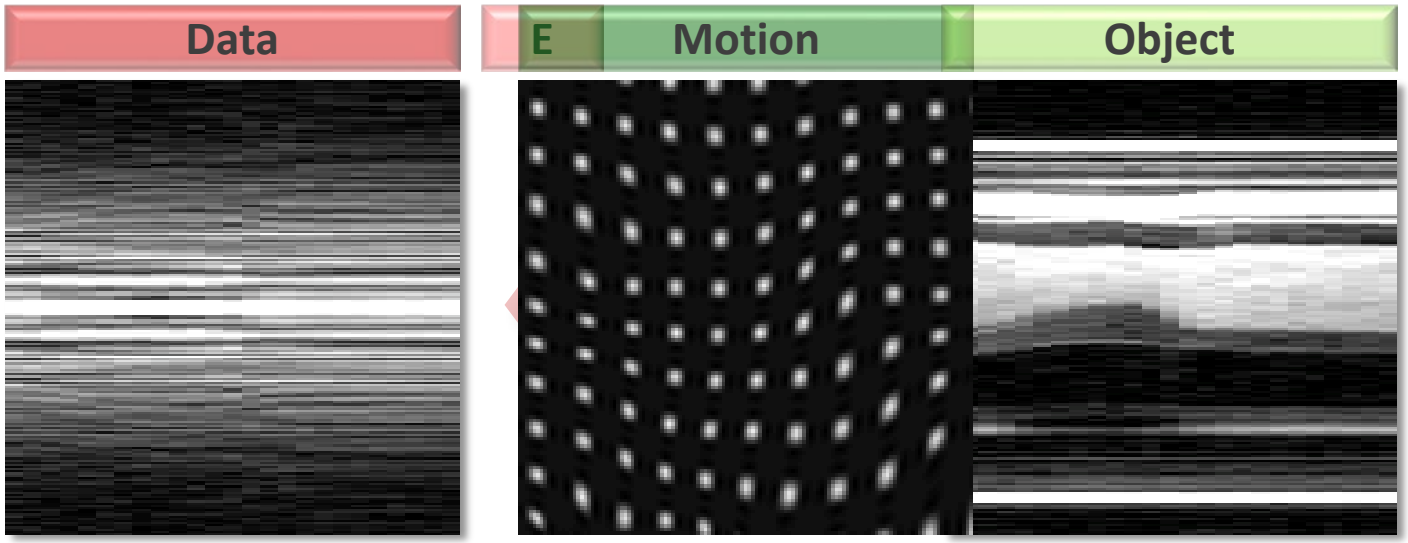

$$\vec{d} = \sum_i E_i T_i \vec{\rho} = \hat{E}$$

$$\vec{i} = \left(\hat{E}^H \Psi^{-1} \hat{E} + \lambda \Theta^{-1}\right)^{-1} \hat{E}^H \Psi^{-1} \vec{d}$$

Batchelor P et al. MRM 2005 Schmidt JF et al. MRM 2011

Data-driven motion correction

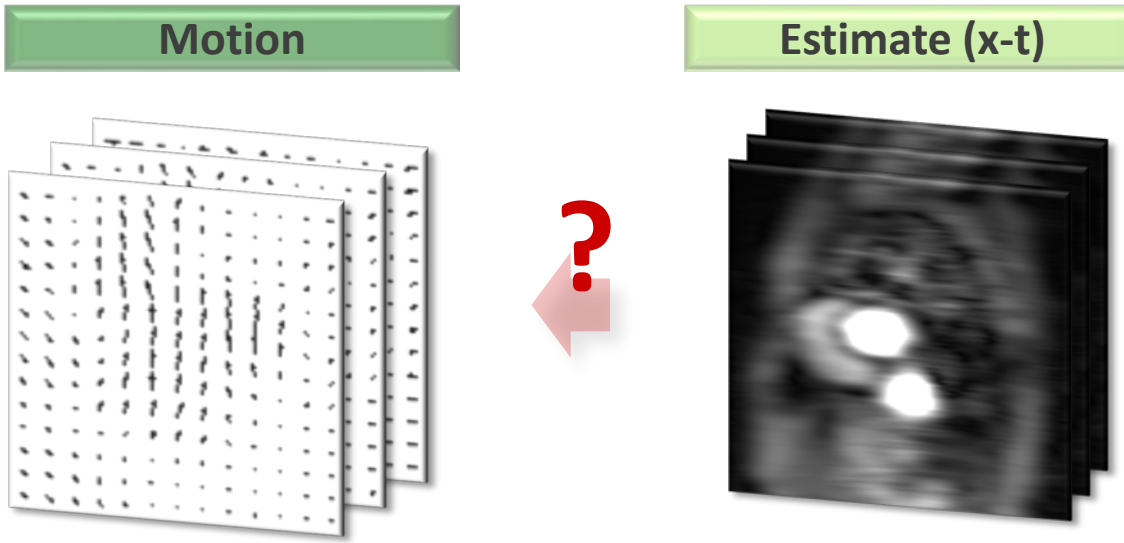

$$\vec{i} \rightarrow \quad \text{argmin}_i \left\| \vec{d} - E \cdot \vec{i} \right\|_2^2 + \lambda \left\| \left({}^{Tx\text{-}pc}\Theta \right)^{-1} B_{f->pc} E_{t->f} \mathbf{Ti} \right\|_2^2$$

k-t PCA^{mc}

Schmidt JF et al. MRM 2013

Data-driven motion correction

10x 3D k-t PCA

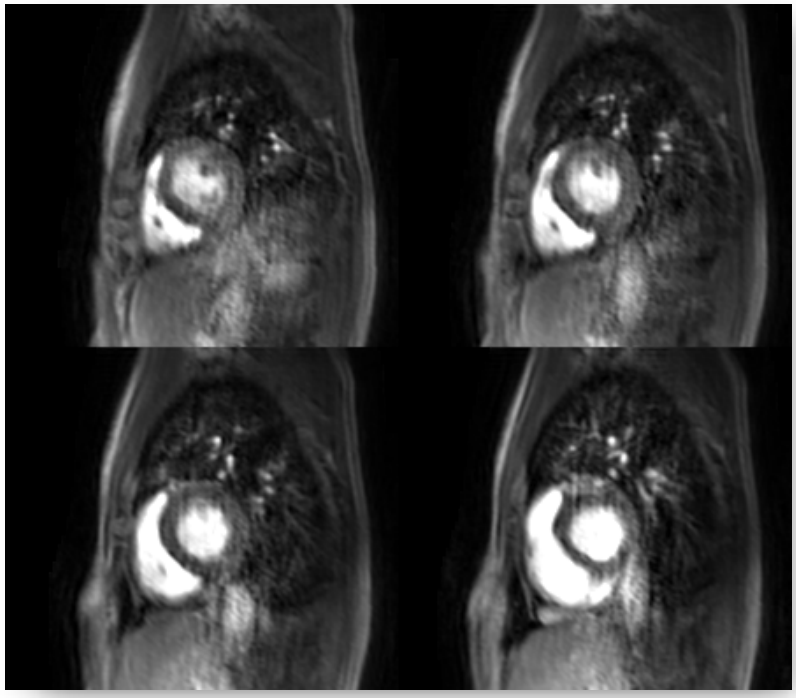

10x 3D k-t PCA^{mc}

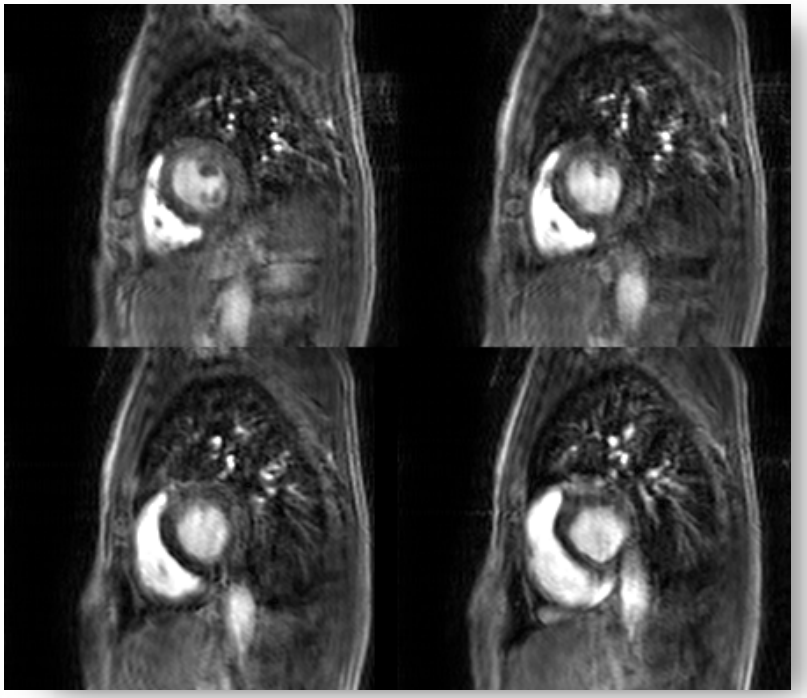

Schmidt JF et al. MRM 2013

Hybrid imaging – MR/CT

3D MR Perfusion + CT Angiography

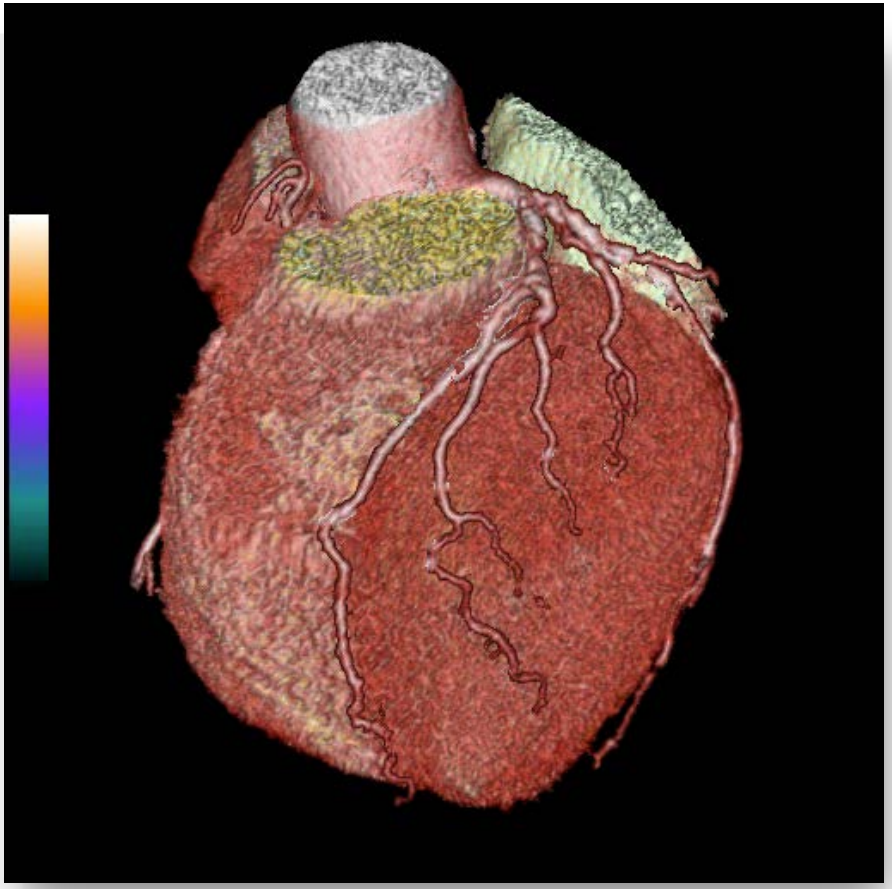

Manka R et al. Eur Heart J 2011

Ischemic cascade

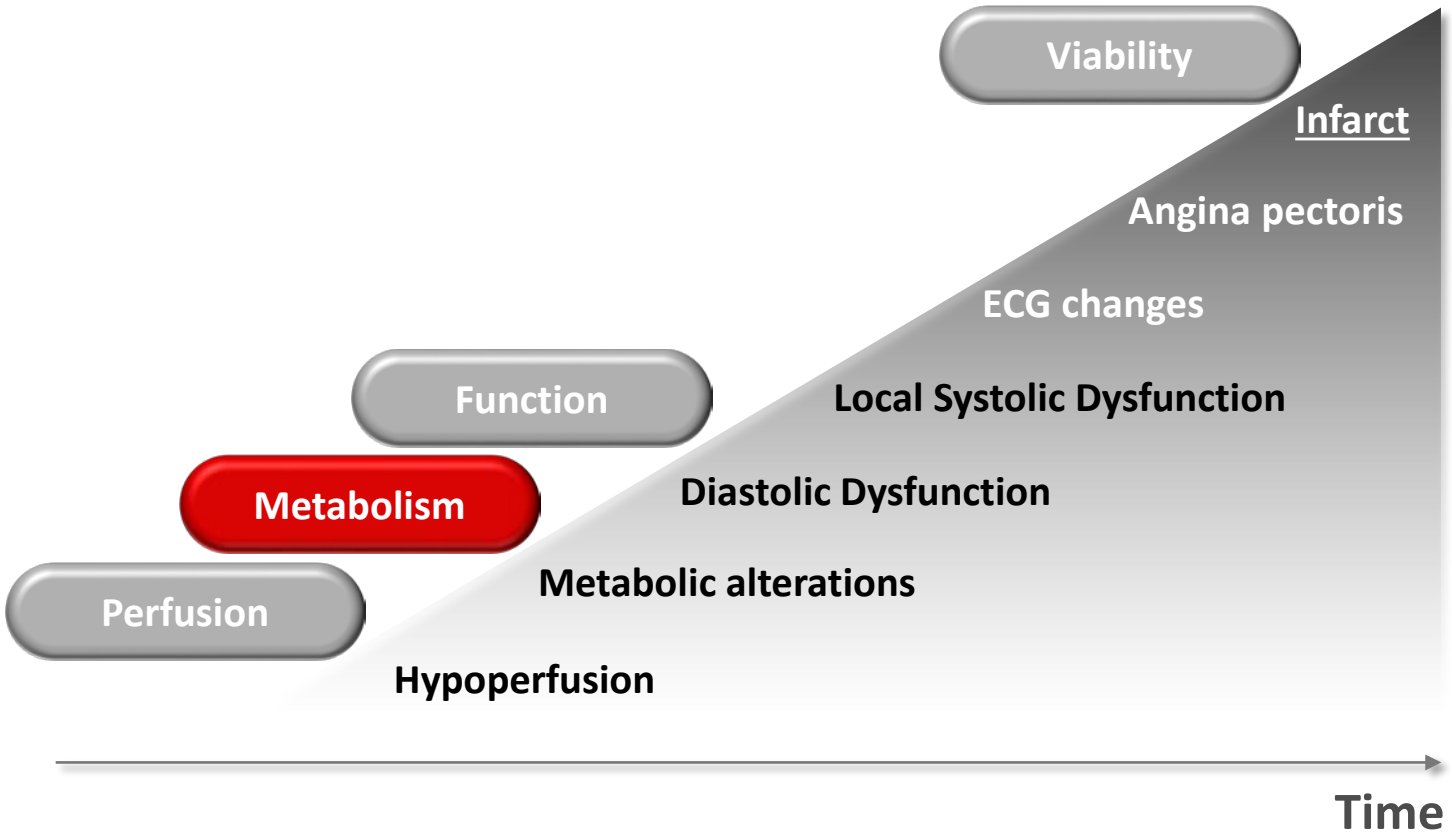

Chemical shift

Radio transmitter

Chemical Shift ➔ Frequency

Signal source

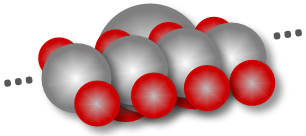

Radio receiver

Magnetic field

Frequency ➔ Chemical Shift

Chemical shift

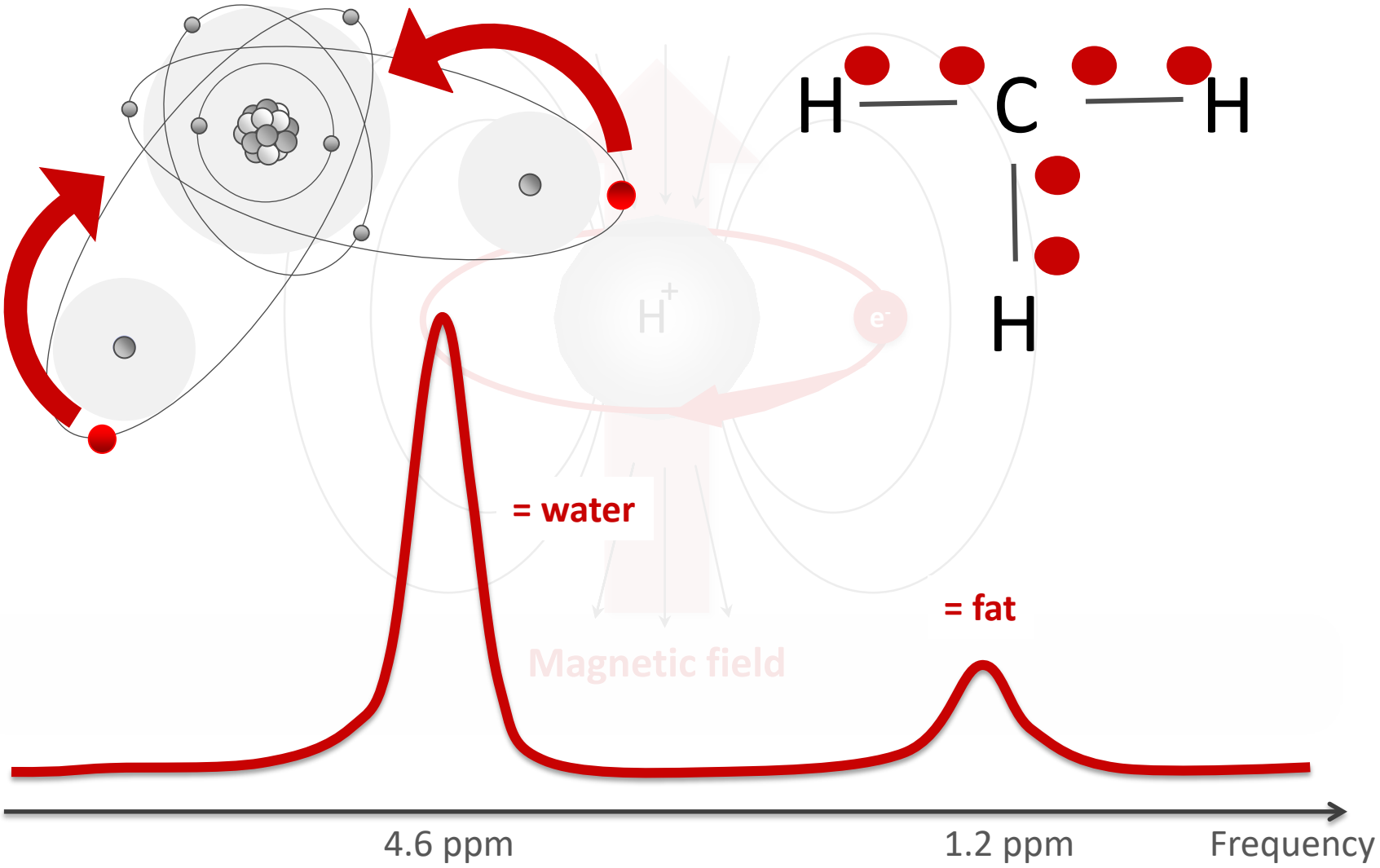

Cell respiration

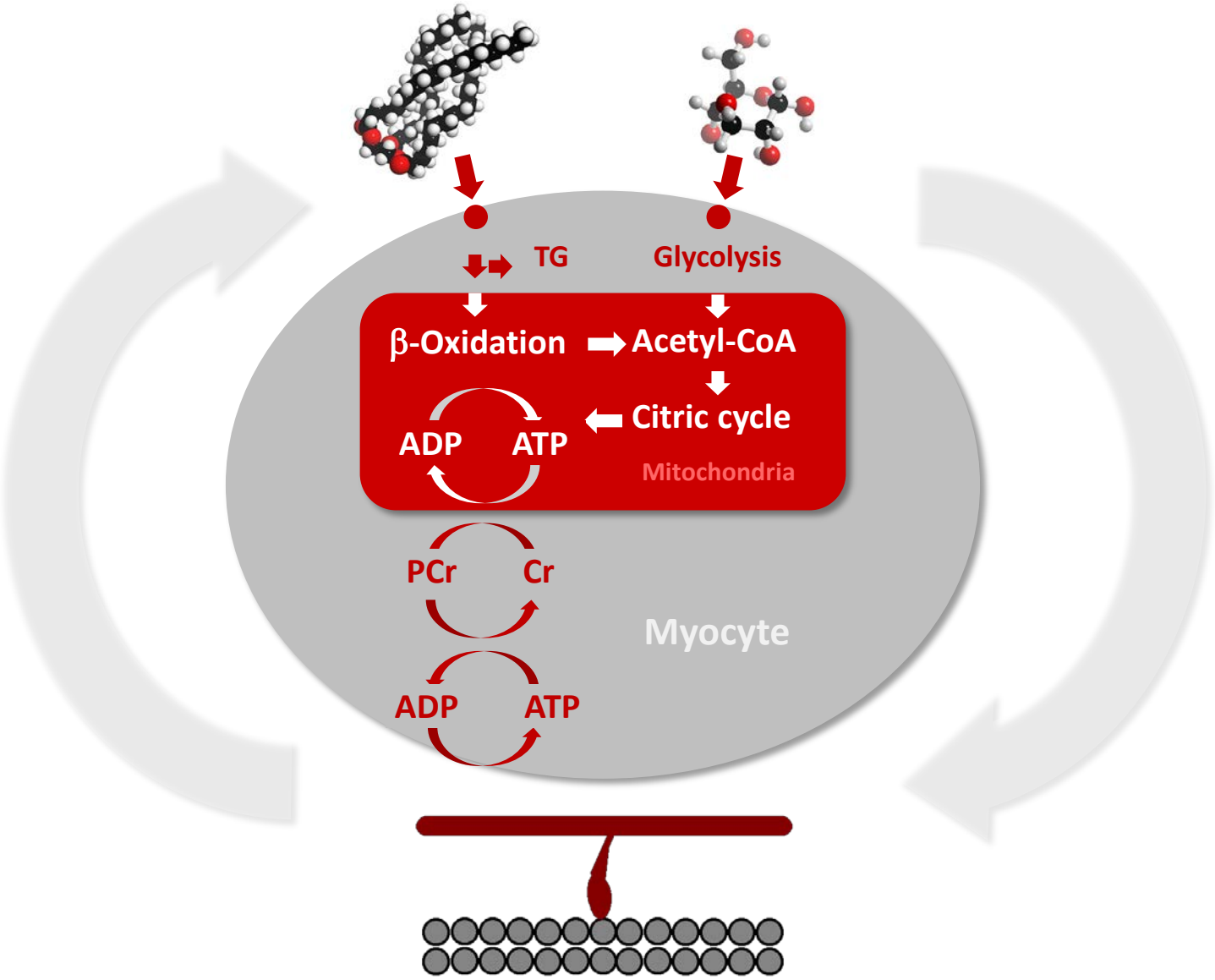

Spectroscopy

Radio transmitter

Position ➔ Frequency

Signal source

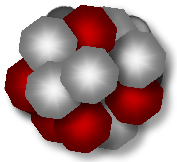

Radio receiver

Magnetic field

Frequency ➔ Position

^{1}H, ^{19}F, ^{31}P, ^{13}C

Carbon imaging

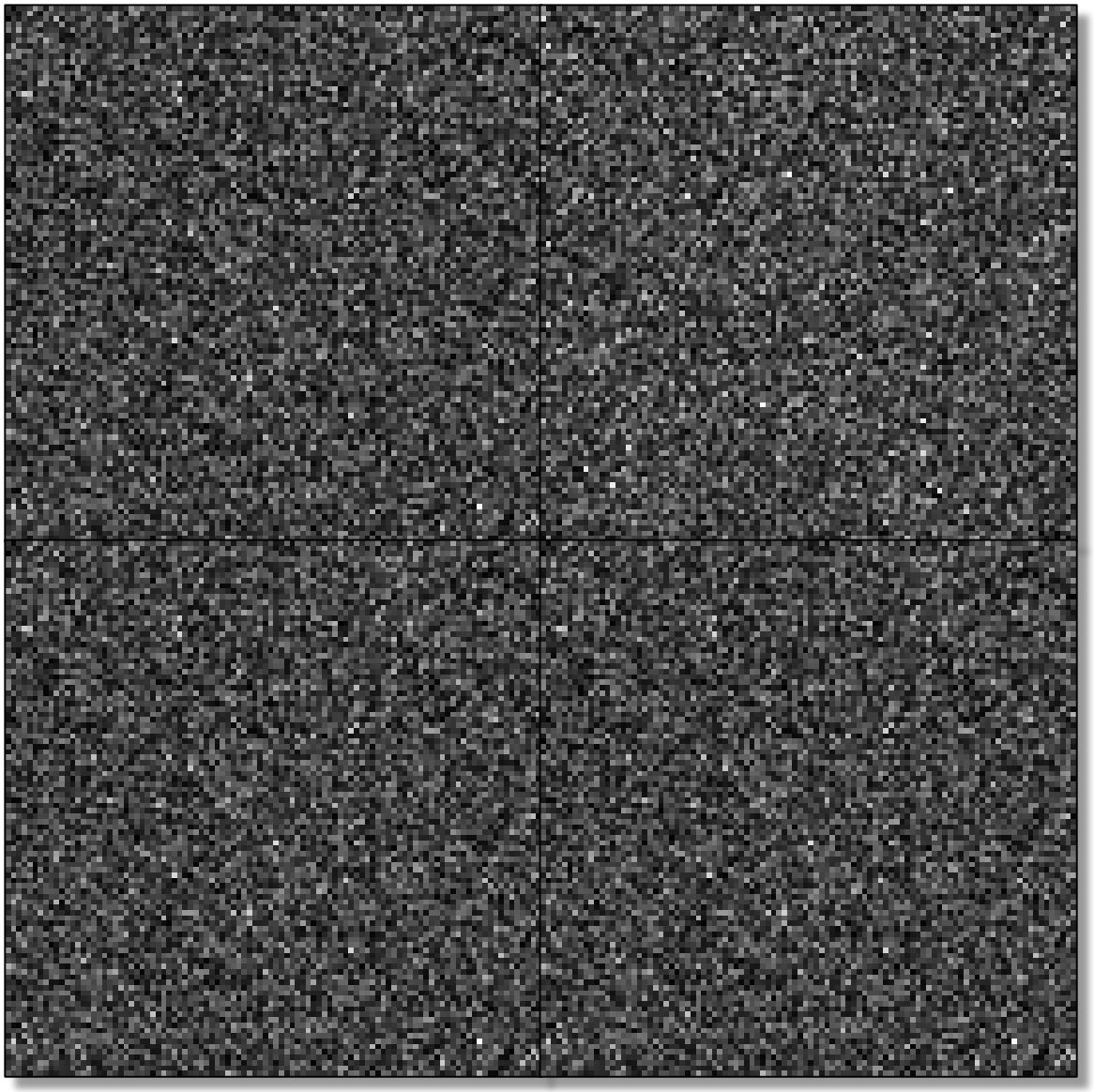

0.1-1 mM

Dynamic Nuclear Polarization

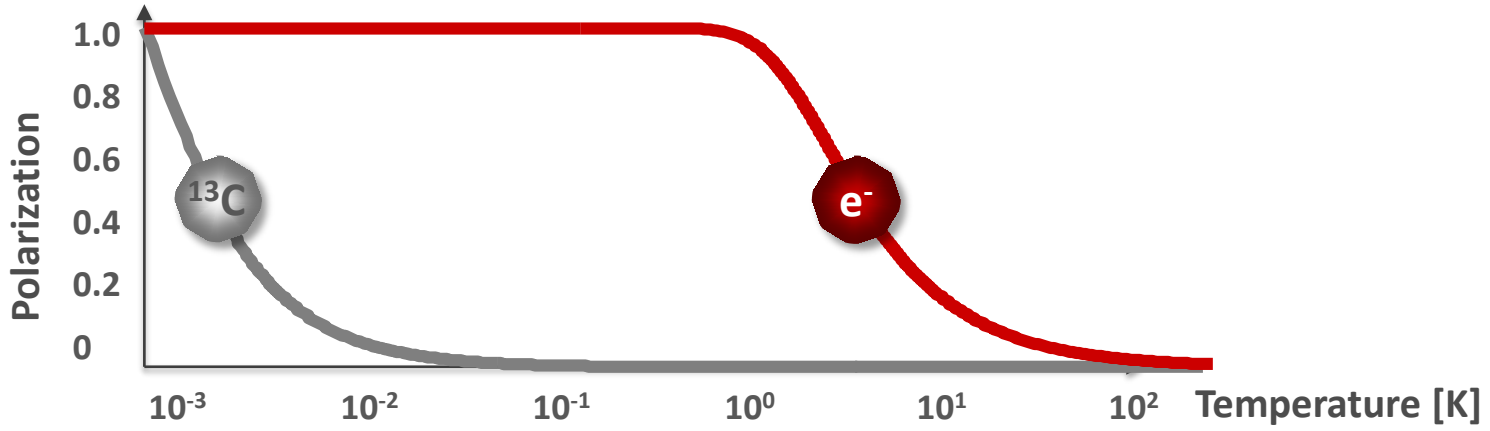

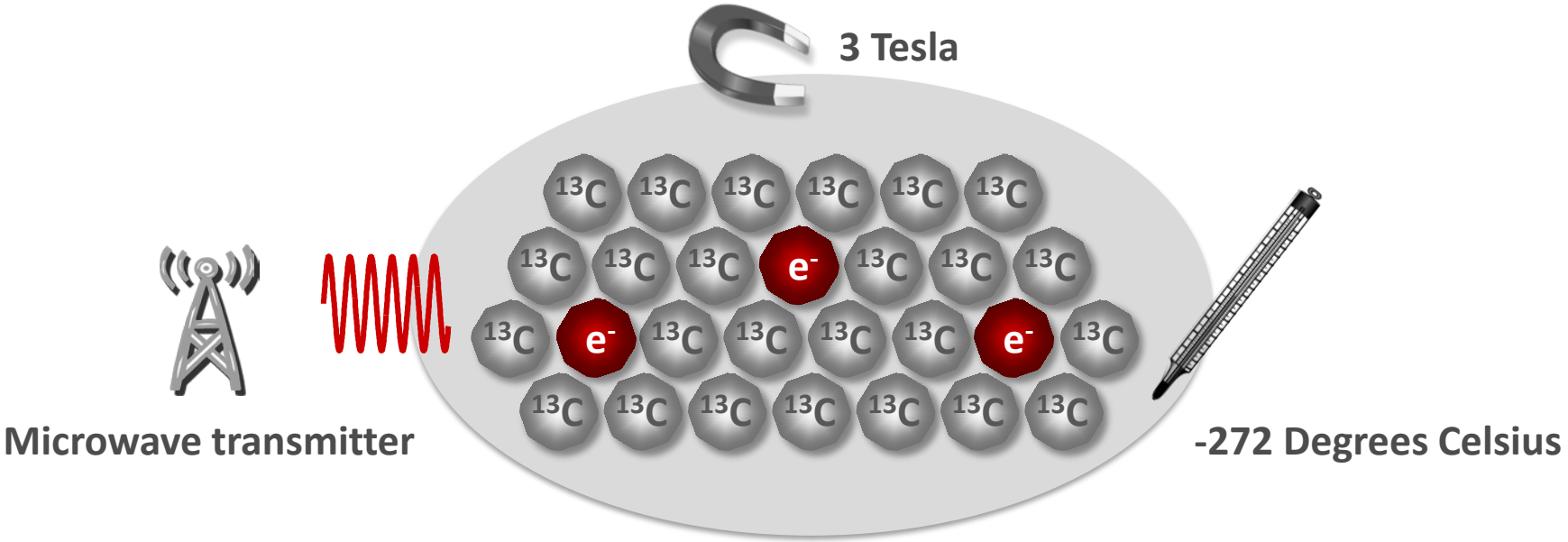

Dissolution Dynamic Nuclear Polarization

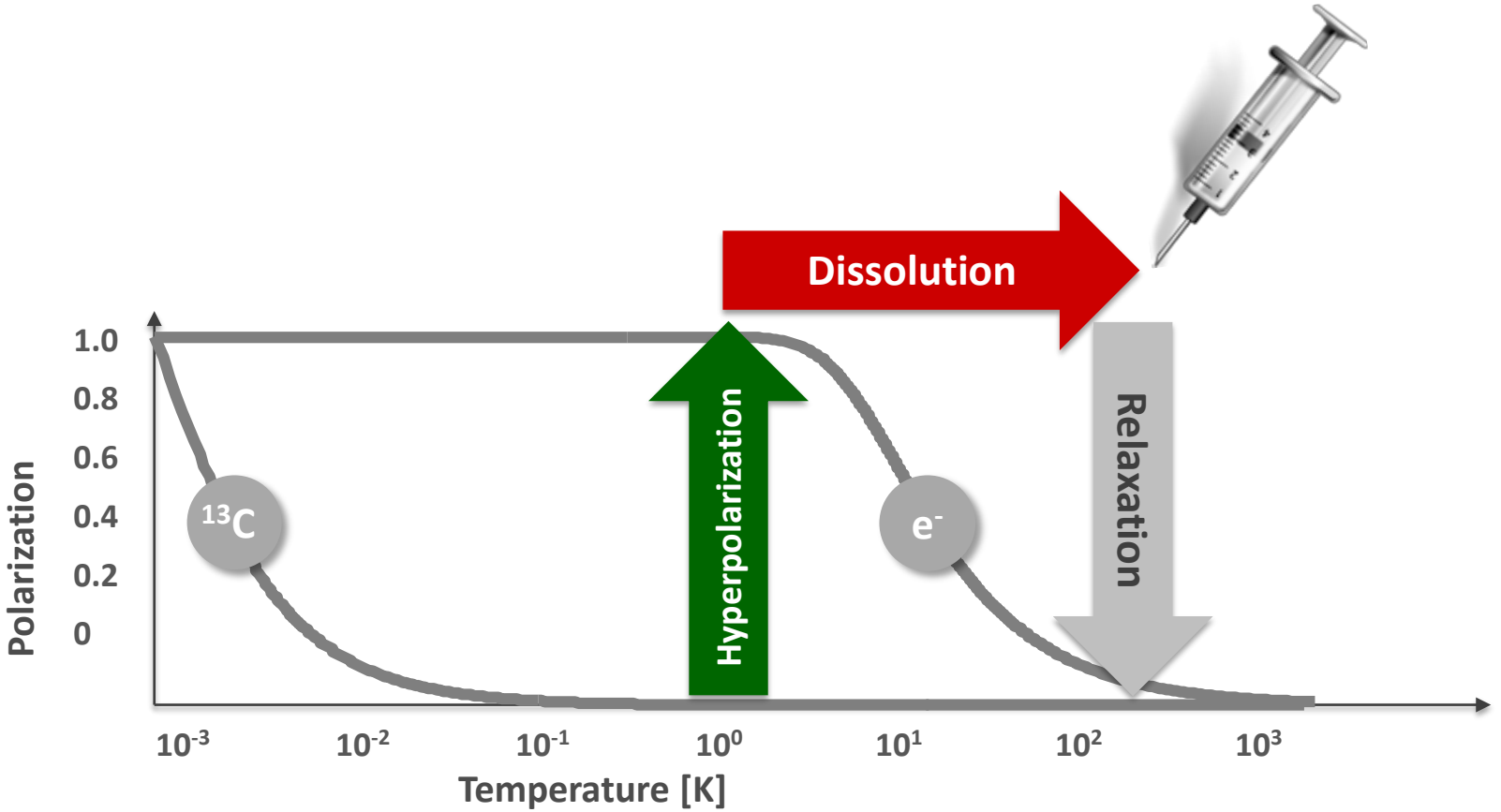

Ardenkjaer-Larsen JH et al. PNAS 2003

Prototype polarizer

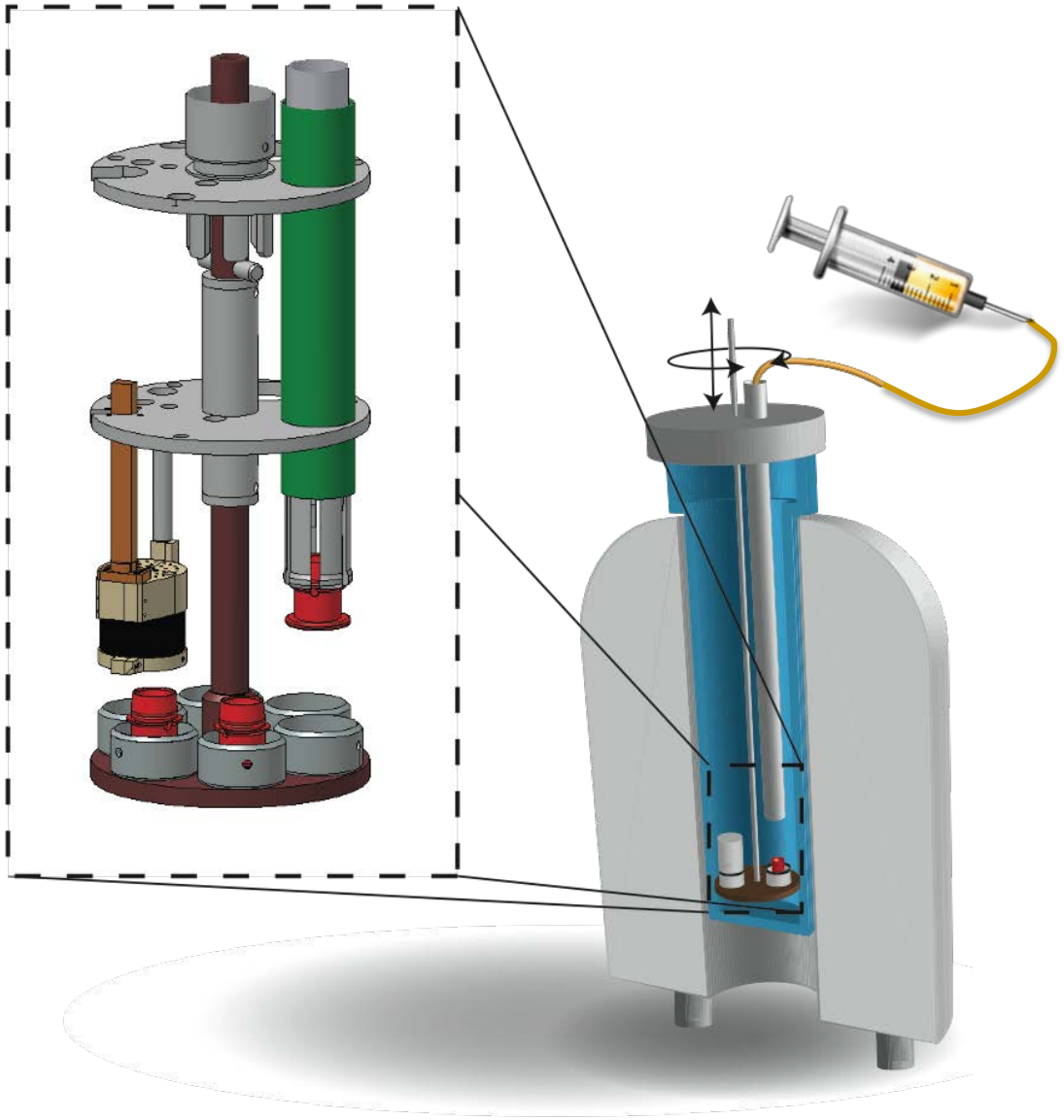

Batel M et al. JMR 2012

Dissolution dynamic nuclear polarization

Wespi P, Steinhauser J et al.

Metabolism of isolated rat heart

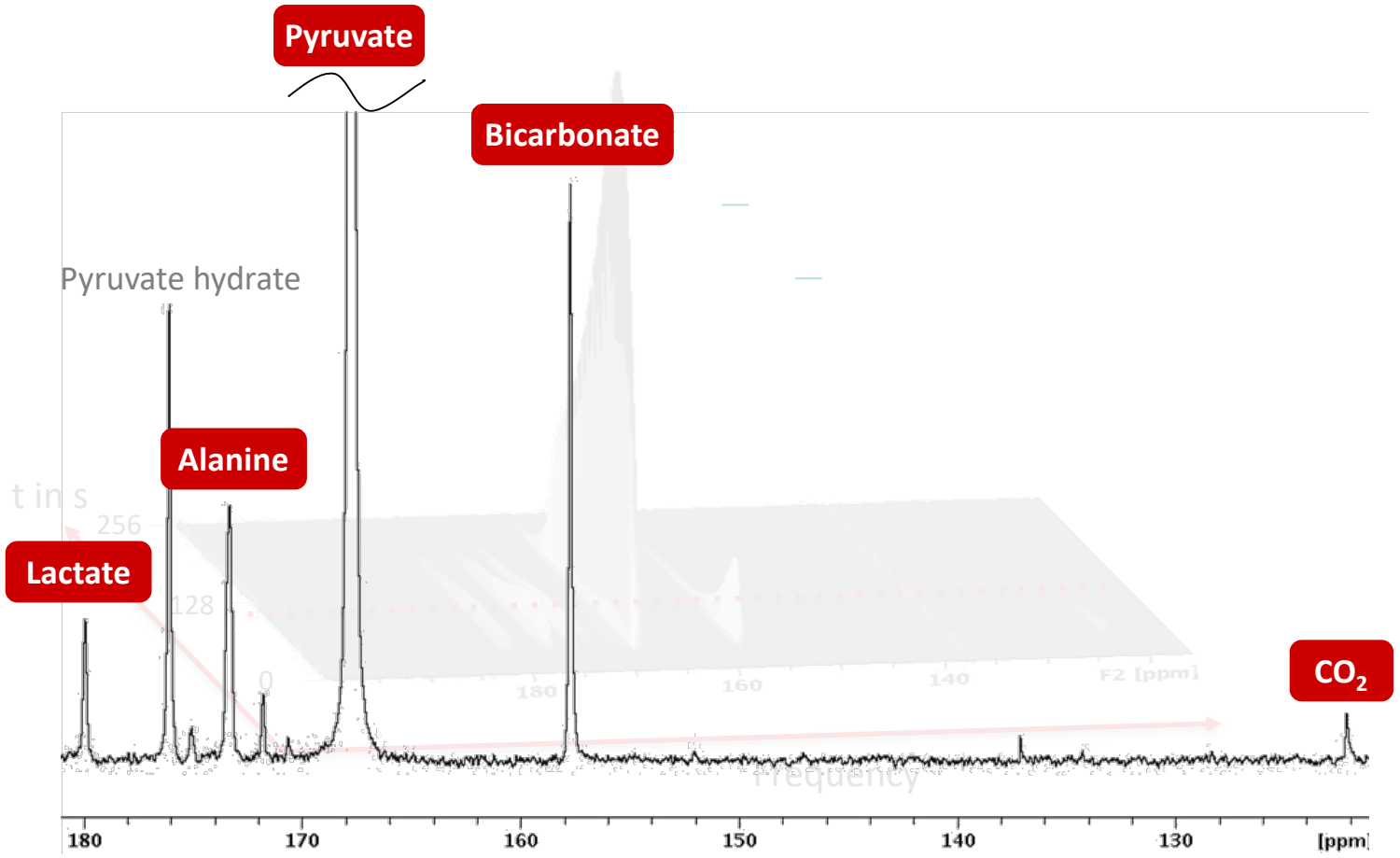

Weiss K et al. JAMR 2012

Real-time metabolic imaging

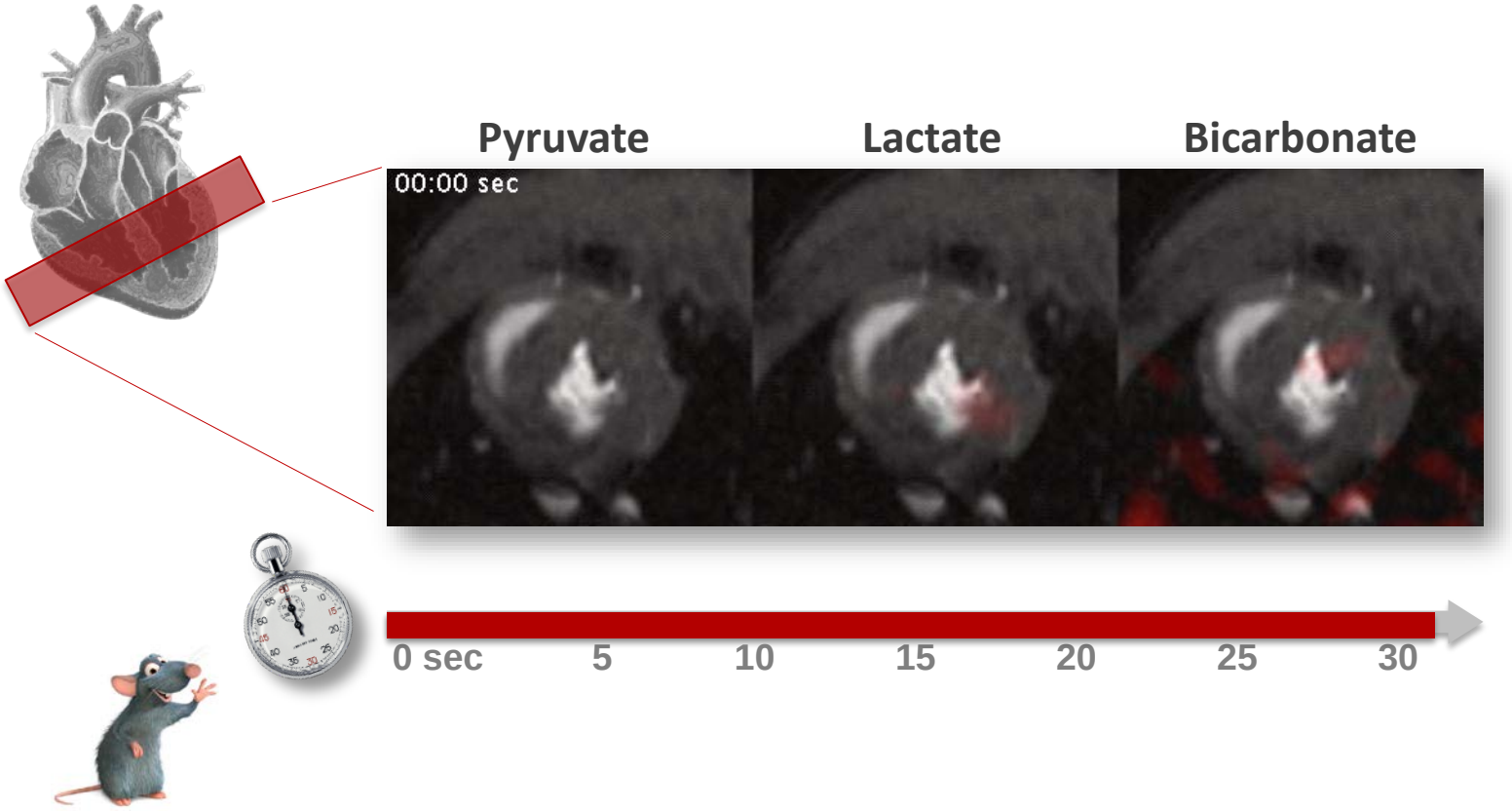

O h-Ici D et al. Radiology 2015

From bench to bedside

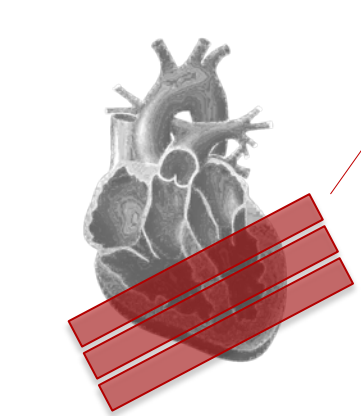

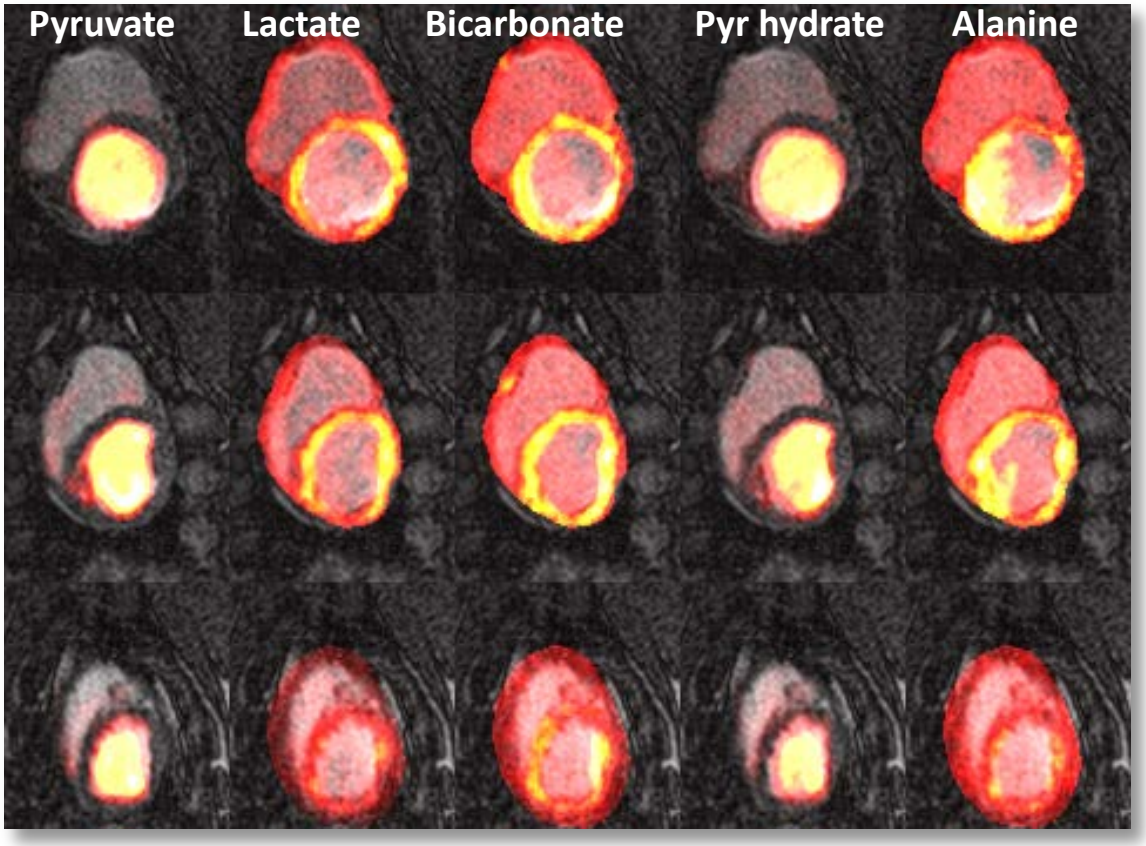

Nelson SJ et al. Science Transl Med 2013

Ischemic cascade

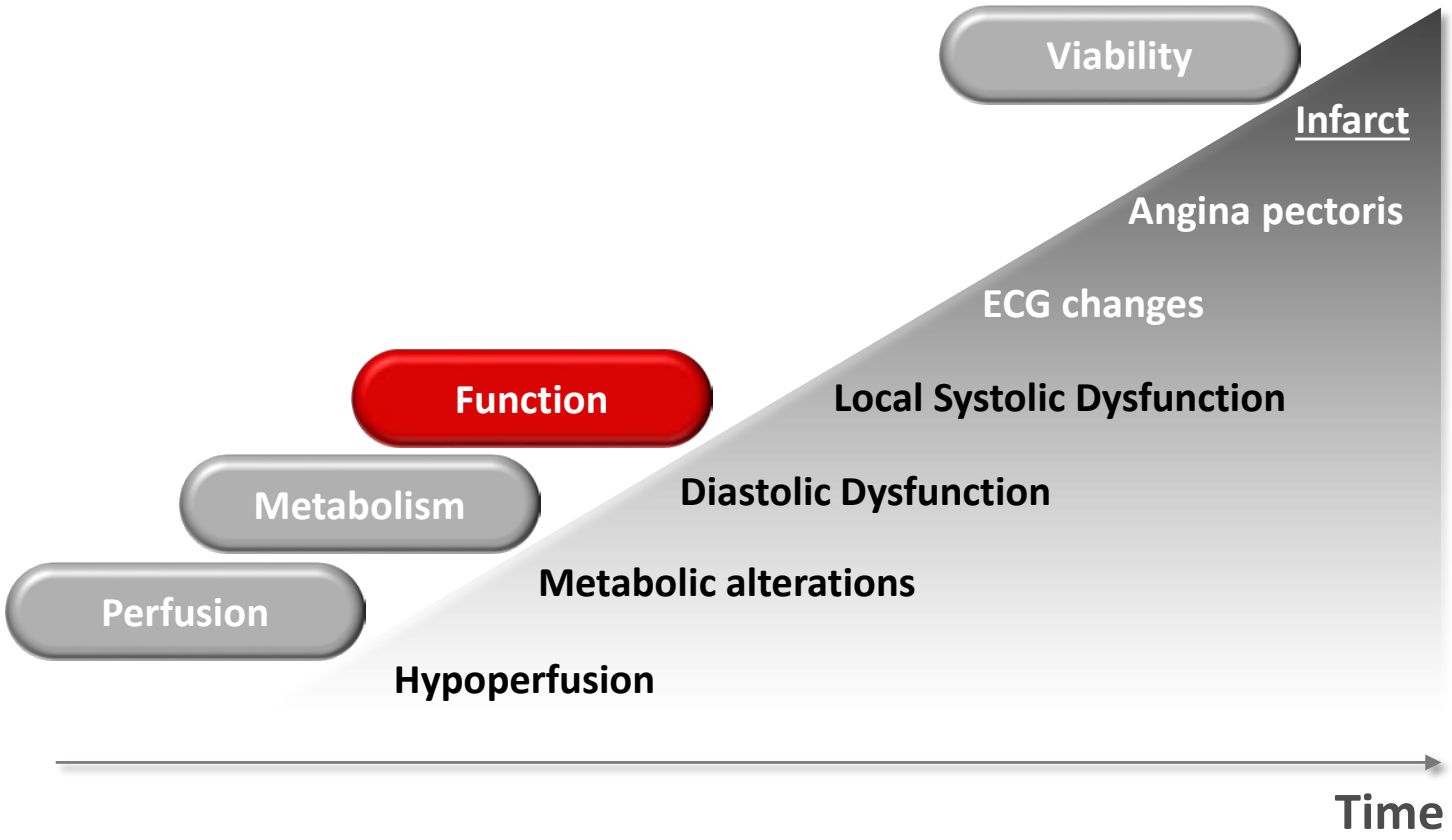

Blood flow

Radio transmitter

Velocity ➔ Phase

Signal sources

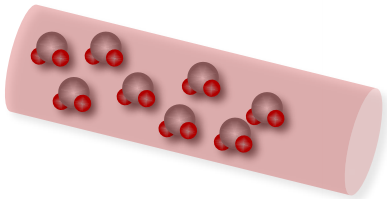

Radio receiver

Magnetic field

Phase ➔ Velocity

Blood flow quantification – relative pressure maps

Flow field

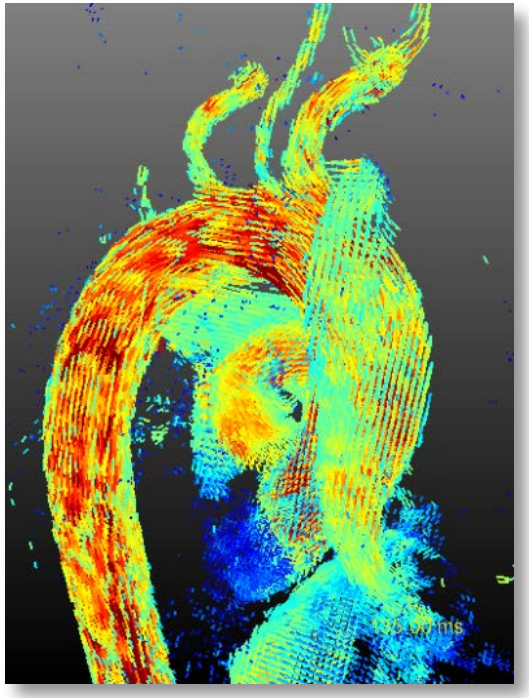

Boundaries

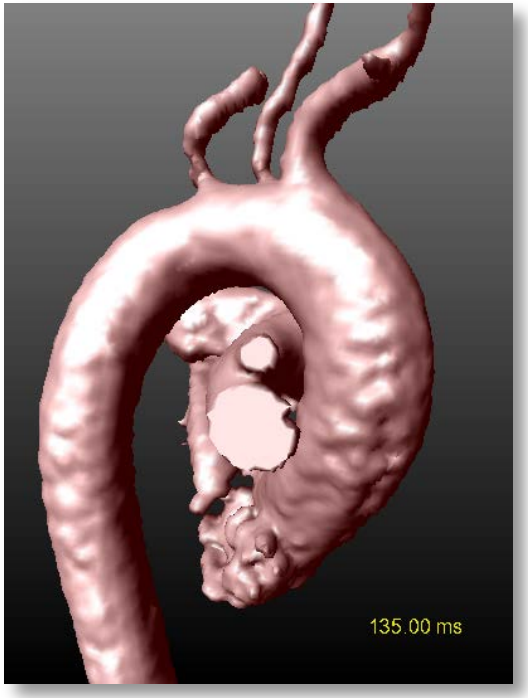

Pressure field

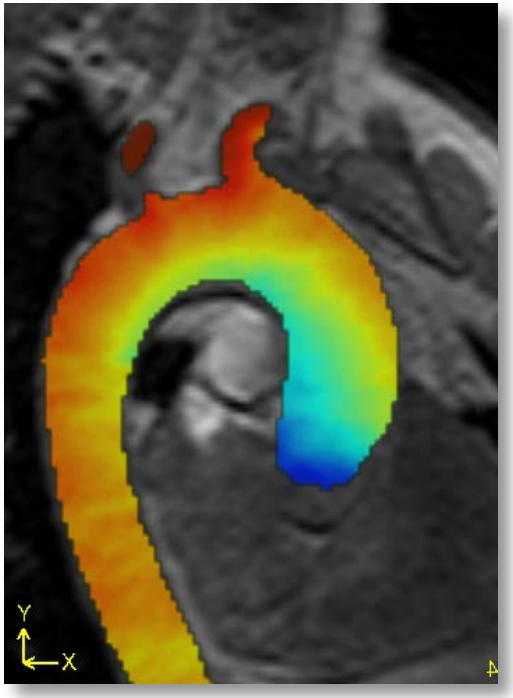

Crelier G et al. GyroTools

Blood flow quantification

Pre operation

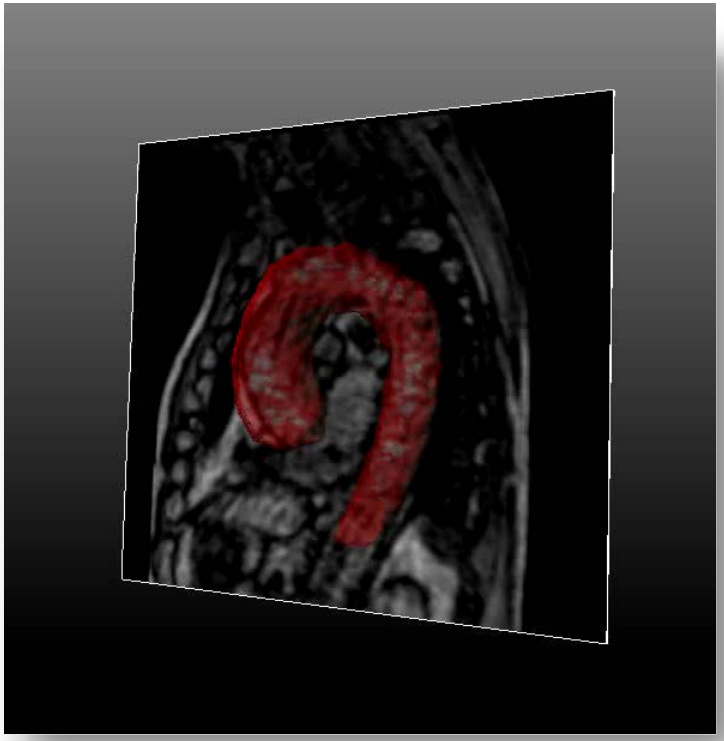

Post operation

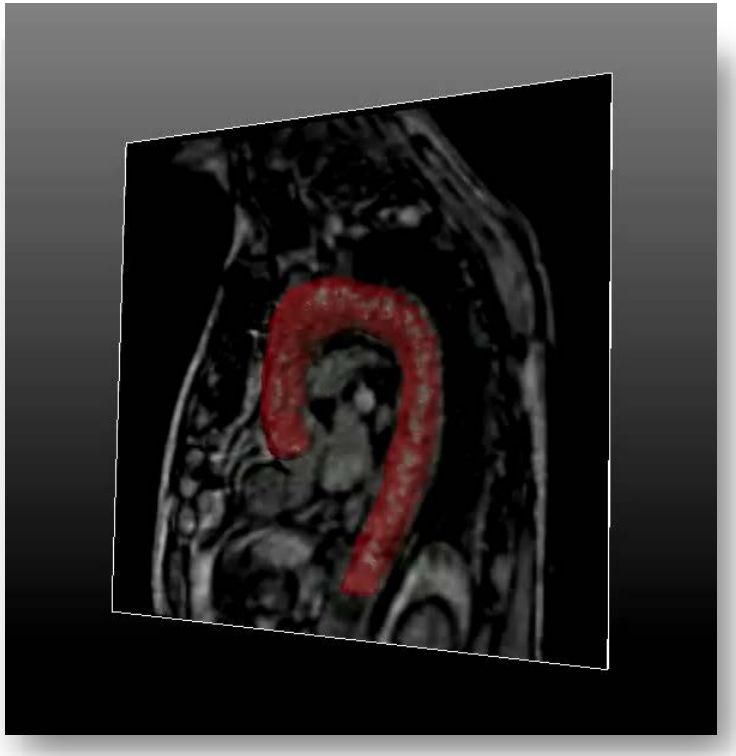

Manka R, Busch J et al. Eur Heart J 2013

Blood flow quantification

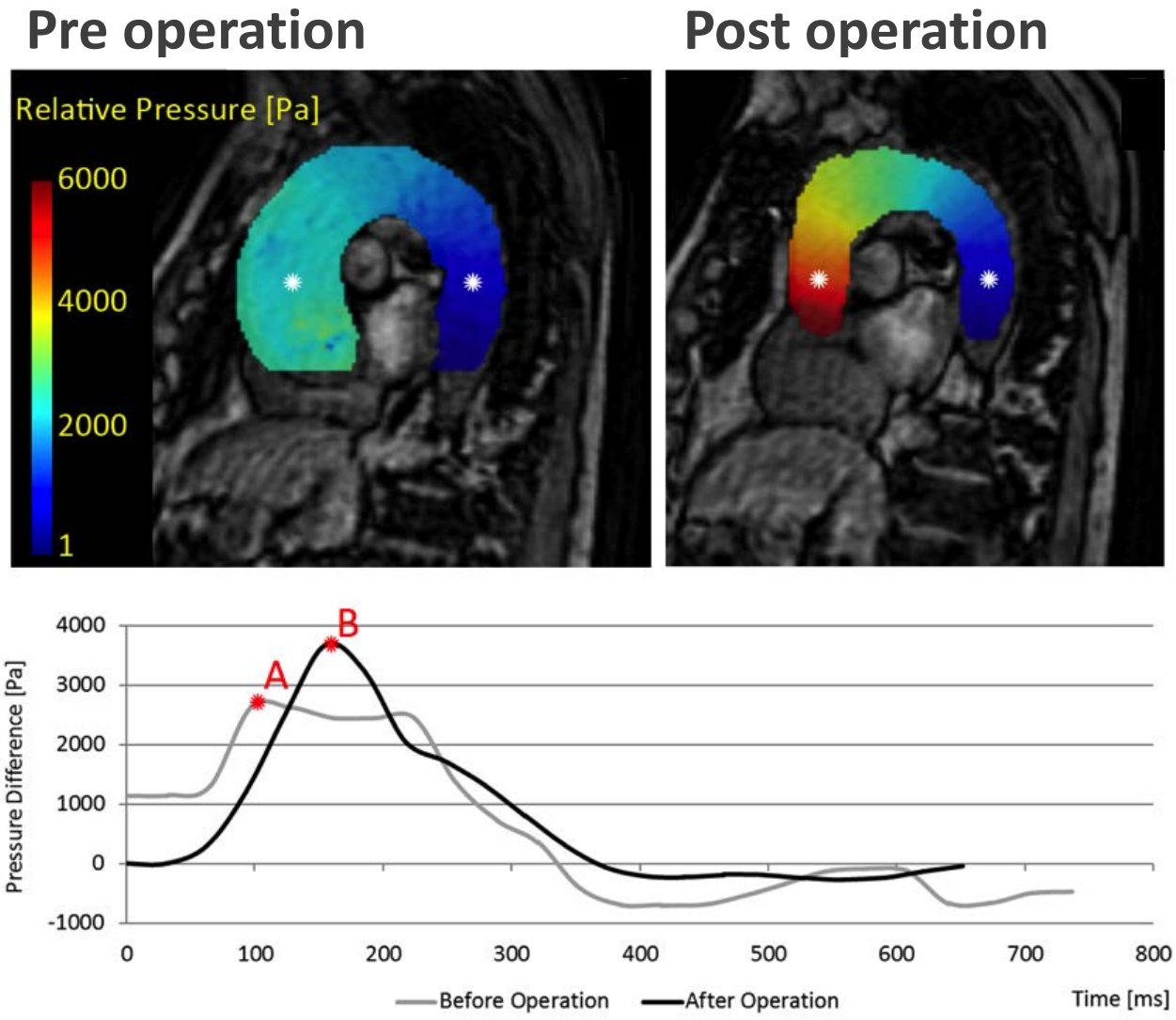

Manka R, Busch J et al. Eur Heart J 2013

Diffusion

Radio transmitter

Position ➔ Frequency

Signal sources

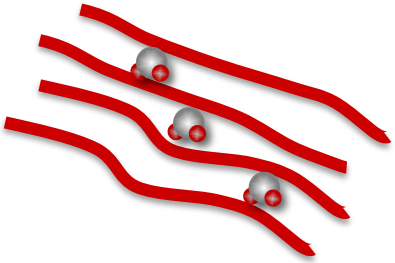

Radio receiver

Magnetic field

Frequency ➔ Position

Velocity compensated diffusion-weighted spin-echo

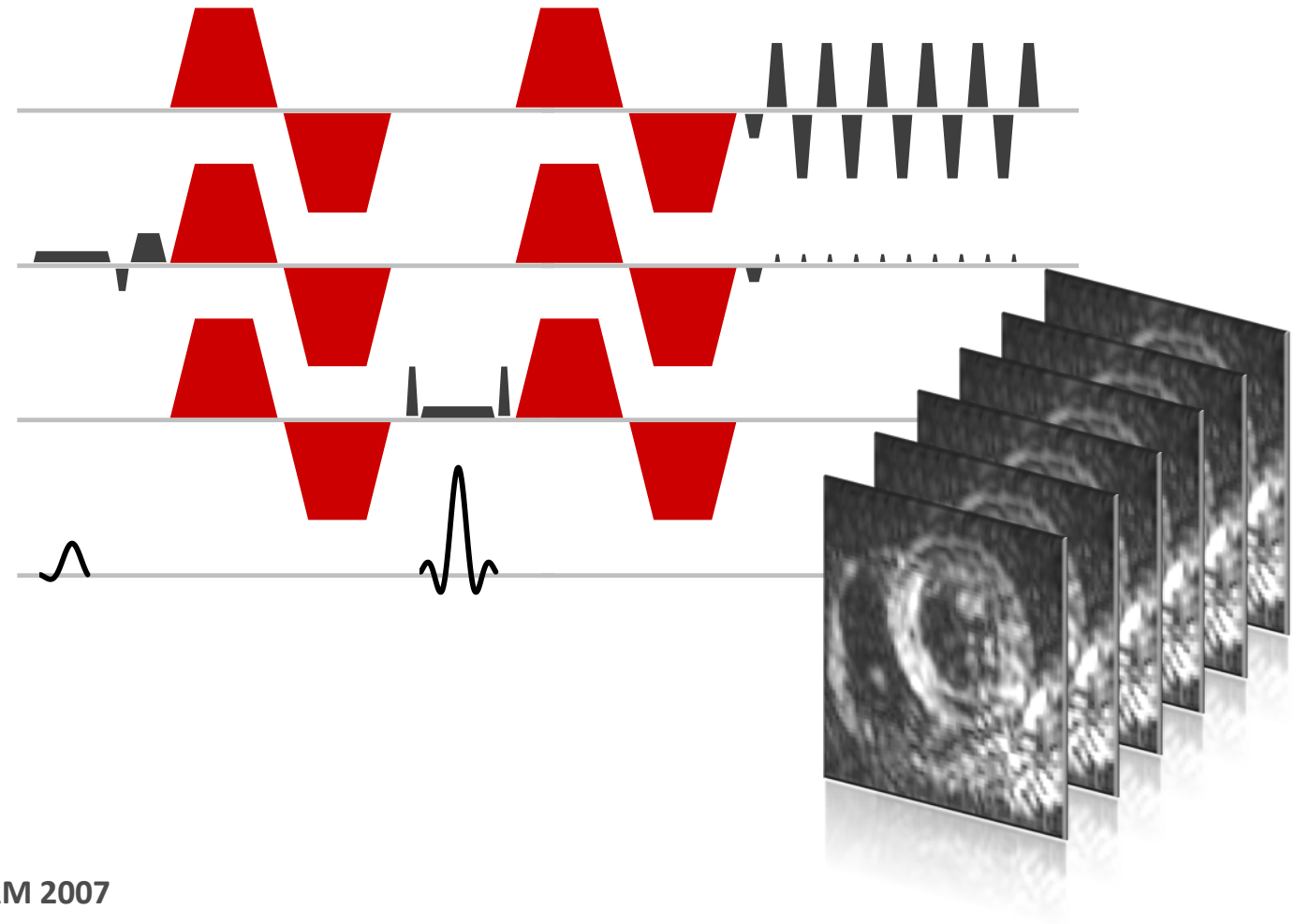

Gamper U et al. MRM 2007

Conformal mapping

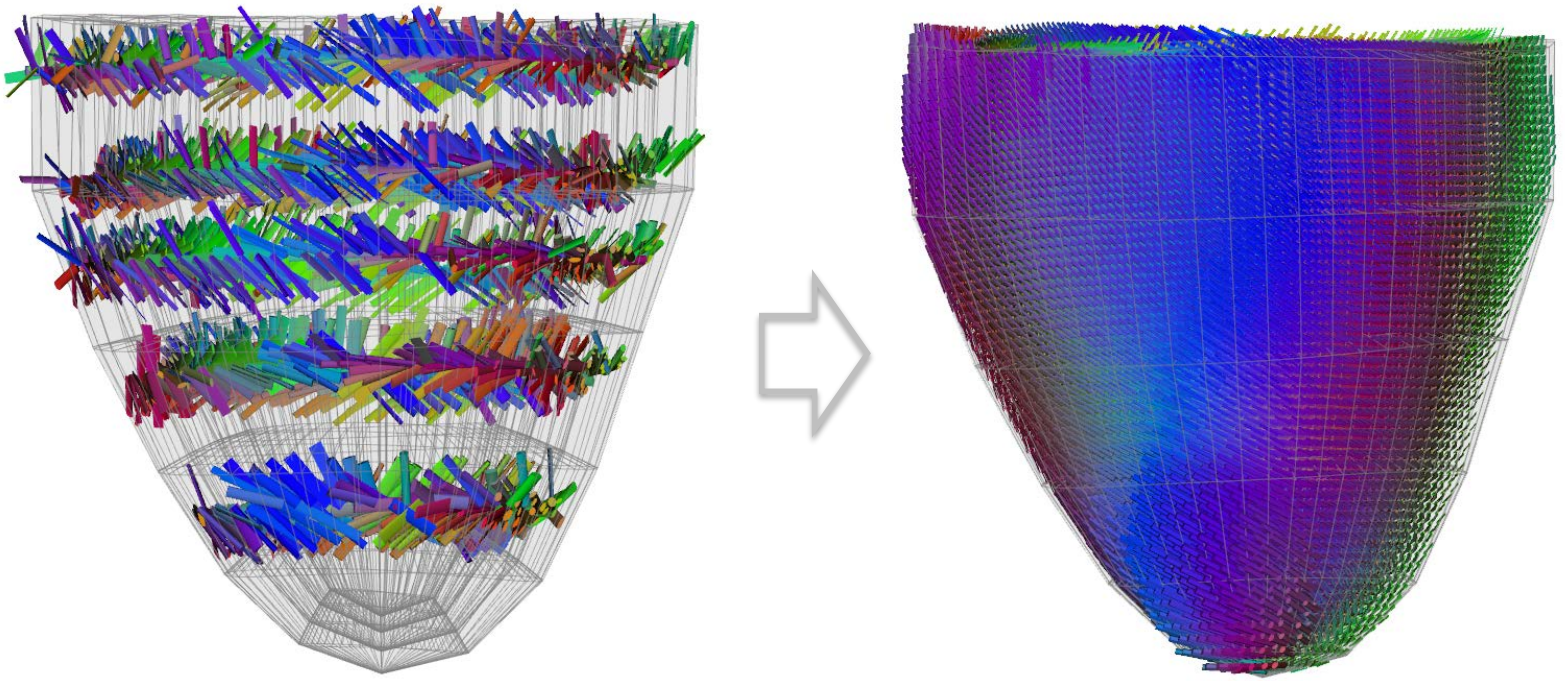

Toussaint N et al. MICCAI 2010

Dynamic Diffusion Tensor Imaging

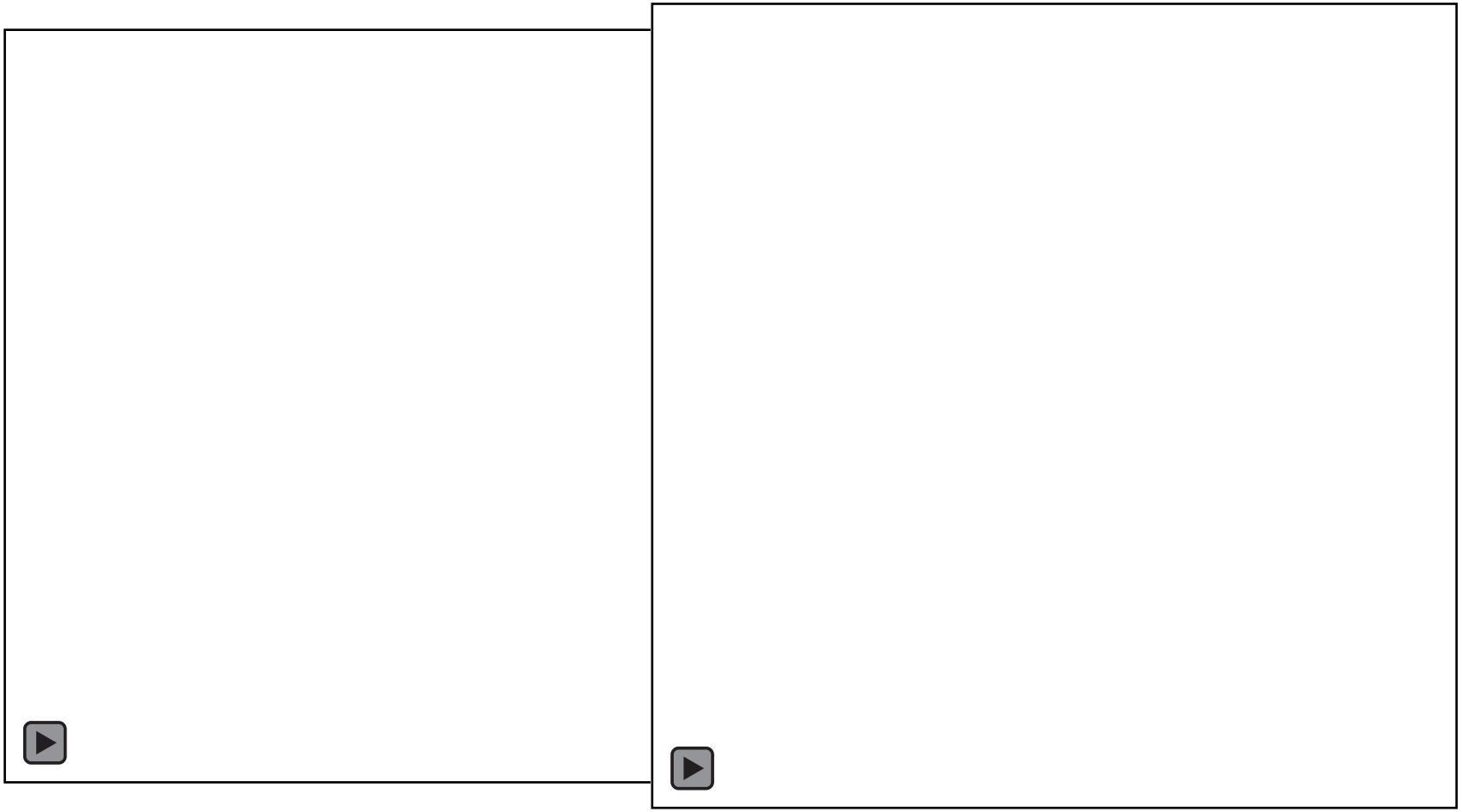

Stoeck C et al. PLOS ONE 2014

Laminar and turbulent flows

Laminar flow

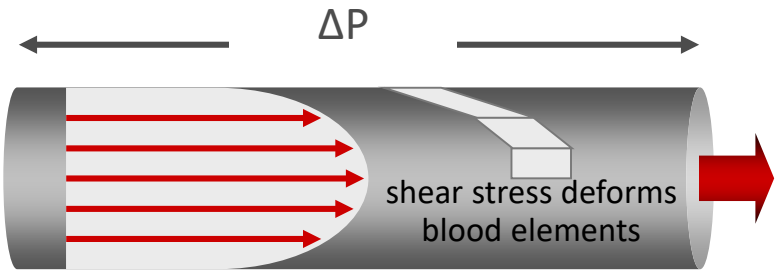

Turbulent flow

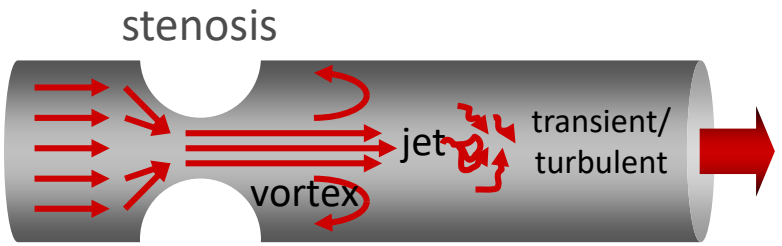

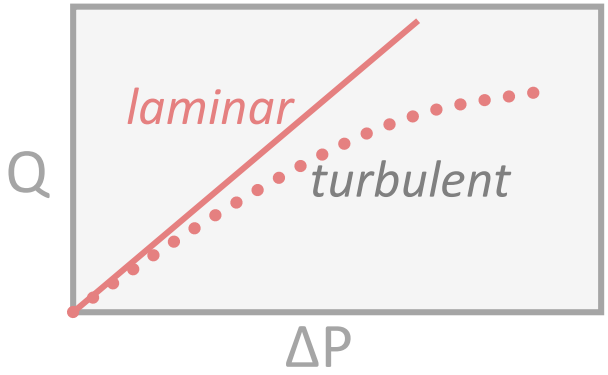

$$\text{ReynoldsNumber} = \frac{\rho v d}{\mu} \propto \frac{\text{Inertialforce}}{\text{Viscousforce}}$$

Universal signal model

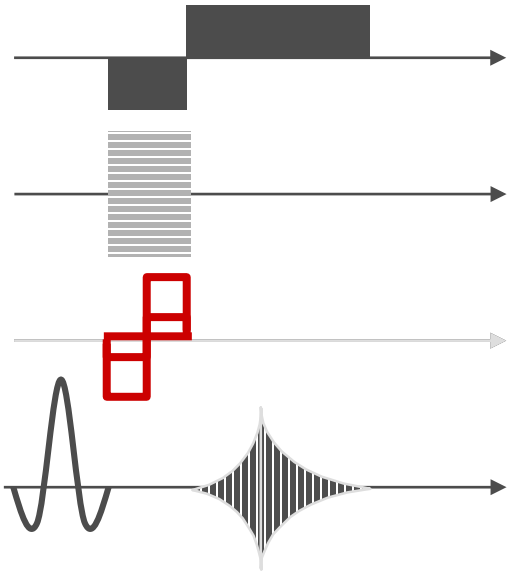

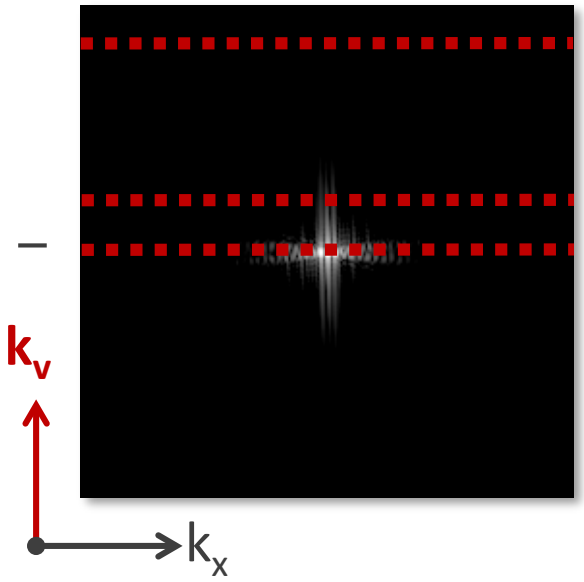

$$S(k_v) = S_0 e^{-\frac{\sigma^2 k_v^2}{2}} e^{i(vk_v+\varphi)}$$

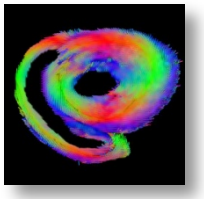

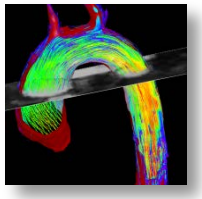

Dyverfeldt P et al. MRM 2006

Bayesian parameter estimation

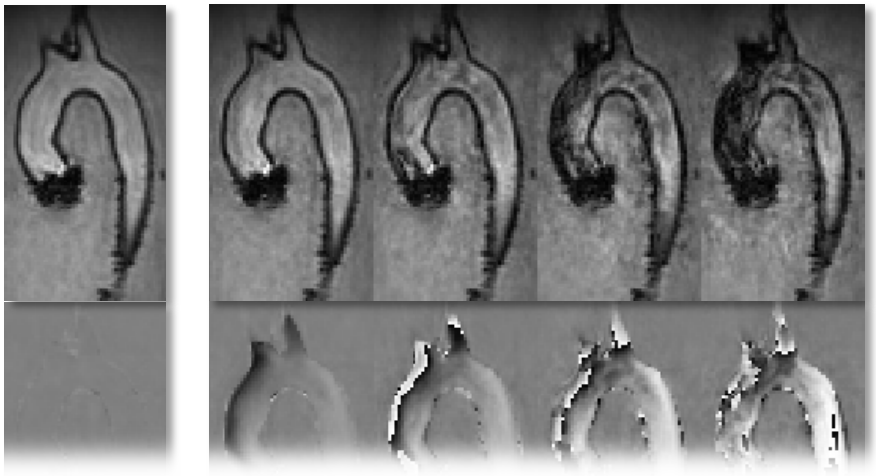

$$P(\boldsymbol{\Theta},\mathbf{B}\,|\,M,I)=\frac{P(\boldsymbol{\Theta},\mathbf{B}\,|\,I)P(M\,|\,\boldsymbol{\Theta},\mathbf{B},I)}{\cancel{P(M\,|\,I)}} \qquad \Theta=[\,\sigma,\,v]$$

Incorporate bounds of parameters

Incorporate knowledge about the noise

$$\iint d\sigma_n d\mathrm{B}$$

$$\boxed{P(\boldsymbol{\Theta}\,|\,M,I)}$$

Binter C et al. MRM 2012

Bayesian multi-point velocity encoding

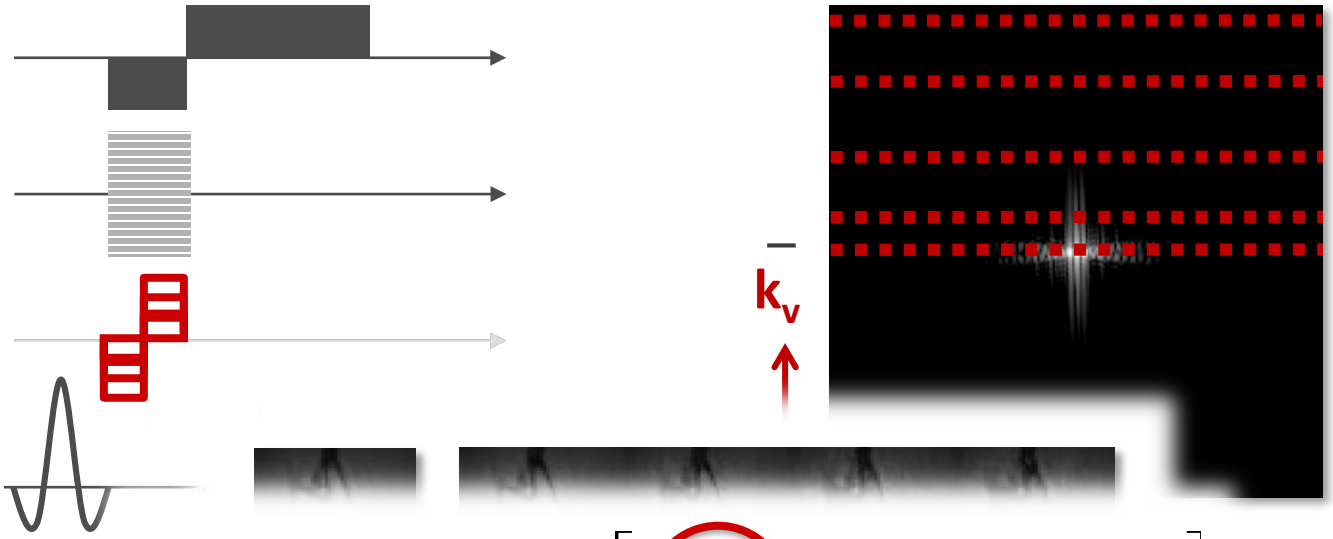

$$\mathrm{Re} = \begin{bmatrix} \delta_{xx} & \tau_{xy} & \tau_{xz} \\ \tau_{yx} & \delta_{yy} & \tau_{yz} \\ \tau_{zx} & \tau_{zy} & \delta_{zz} \end{bmatrix} = \rho \begin{bmatrix} \langle v'^2_1 \rangle & \langle v'_1 v'_2 \rangle & \langle v'_1 v'_3 \rangle \\ \langle v'_1 v'_2 \rangle & \langle v'^2_2 \rangle & \langle v'_2 v'_3 \rangle \\ \langle v'_1 v'_3 \rangle & \langle v'_2 v'_3 \rangle & \langle v'^2_3 \rangle \end{bmatrix}$$

$$\mathrm{TKE} = \frac{\rho}{2} \sum_{i=1}^{3} \langle v'^2_i \rangle = \frac{\rho}{2} \sum_{i=1}^{3} \sigma_i^2$$

Binter C et al. MRM 2012

Aortic valves in-vitro

St. Judes Medical®

Edwards® Sapien

v [cm/s]

TKE [J/m³]

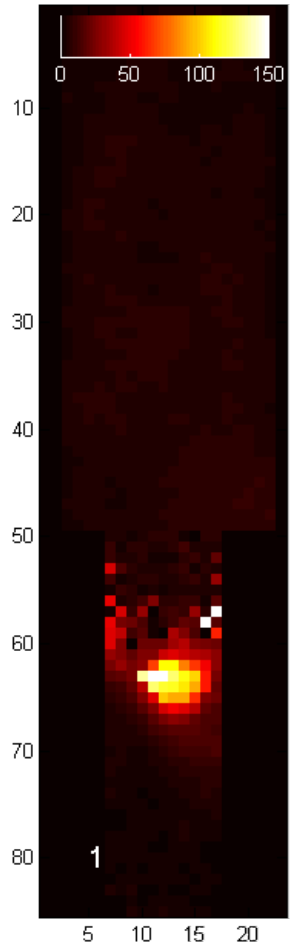

v [cm/s]

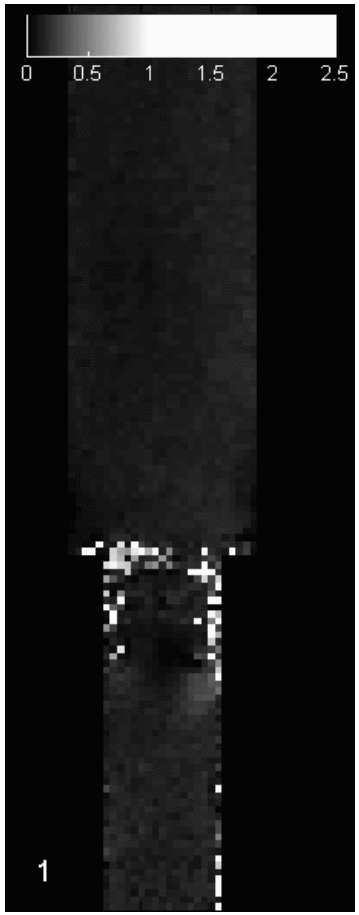

TKE [J/m³]

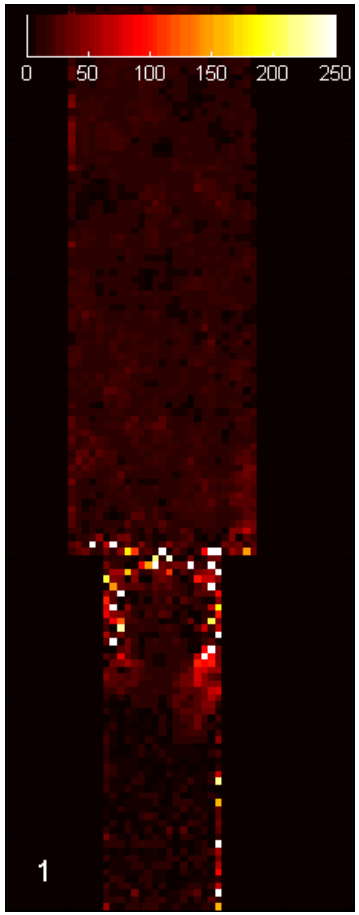

Binter C et al. SCMR 2012

Aortic valves in-vivo

Aortic Stenosis

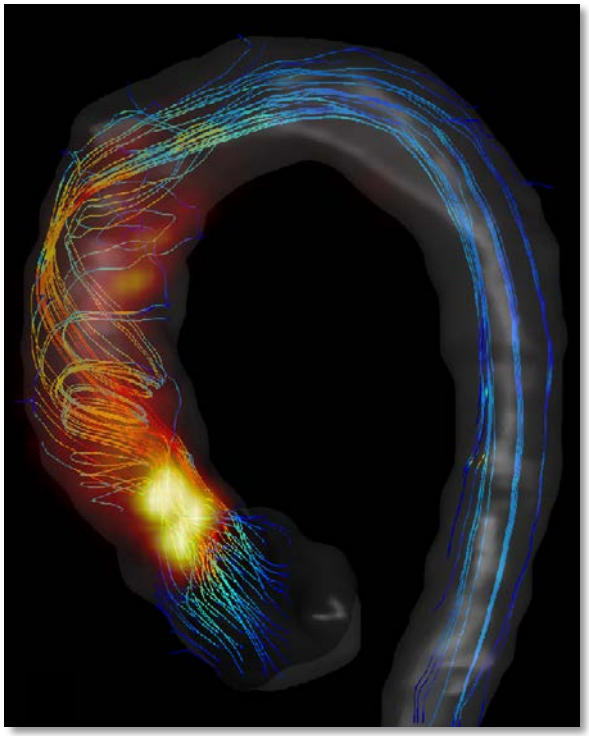

TKE_{peak} 940 J/m³
V_{peak} 3.3 m/s

TAVI

TKE_{peak} 540 J/m³
V_{peak} 2.4 m/s

Healthy

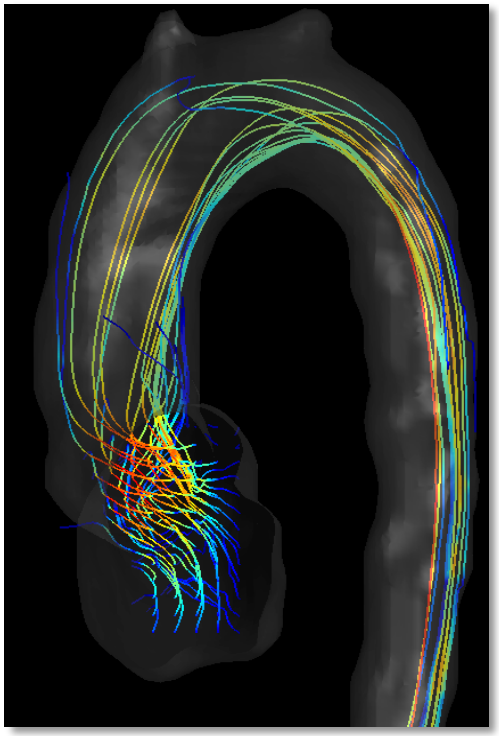

TKE_{peak} 150 J/m³
V_{peak} 1.3 m/s

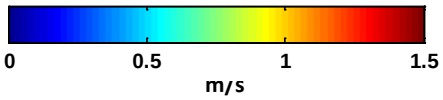

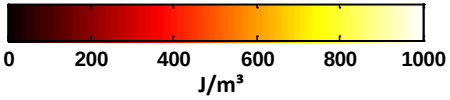

Binter C et al. SCMR 2012

Energy Loss index

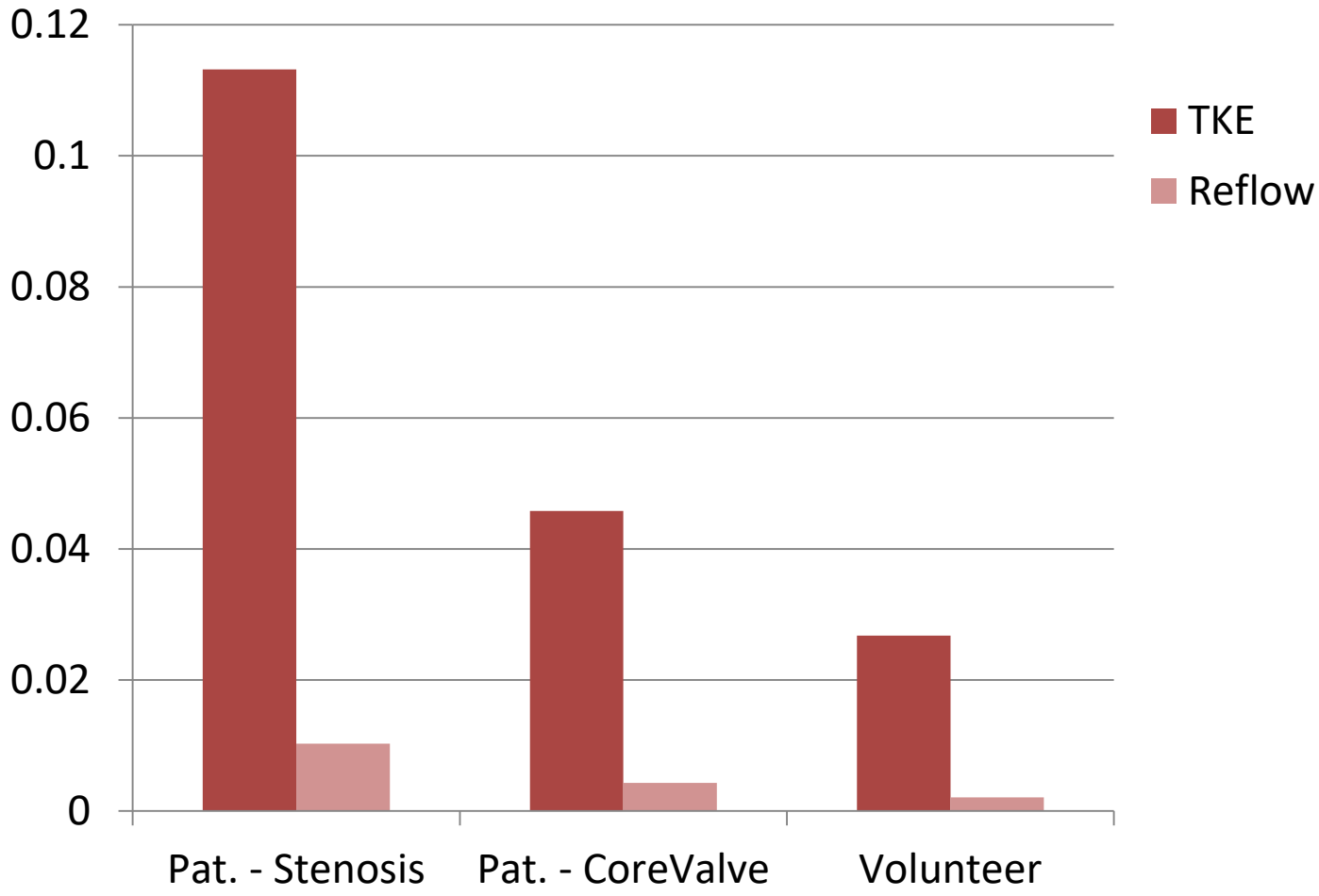

Energy Loss index

$$ELi = \left(\frac{TKE \cdot voxelsize_{z-dir.}}{MKE} + RF \right) \cdot \frac{1}{1 - RF}$$

Binter C et al. SCMR 2012

Image guided simulations

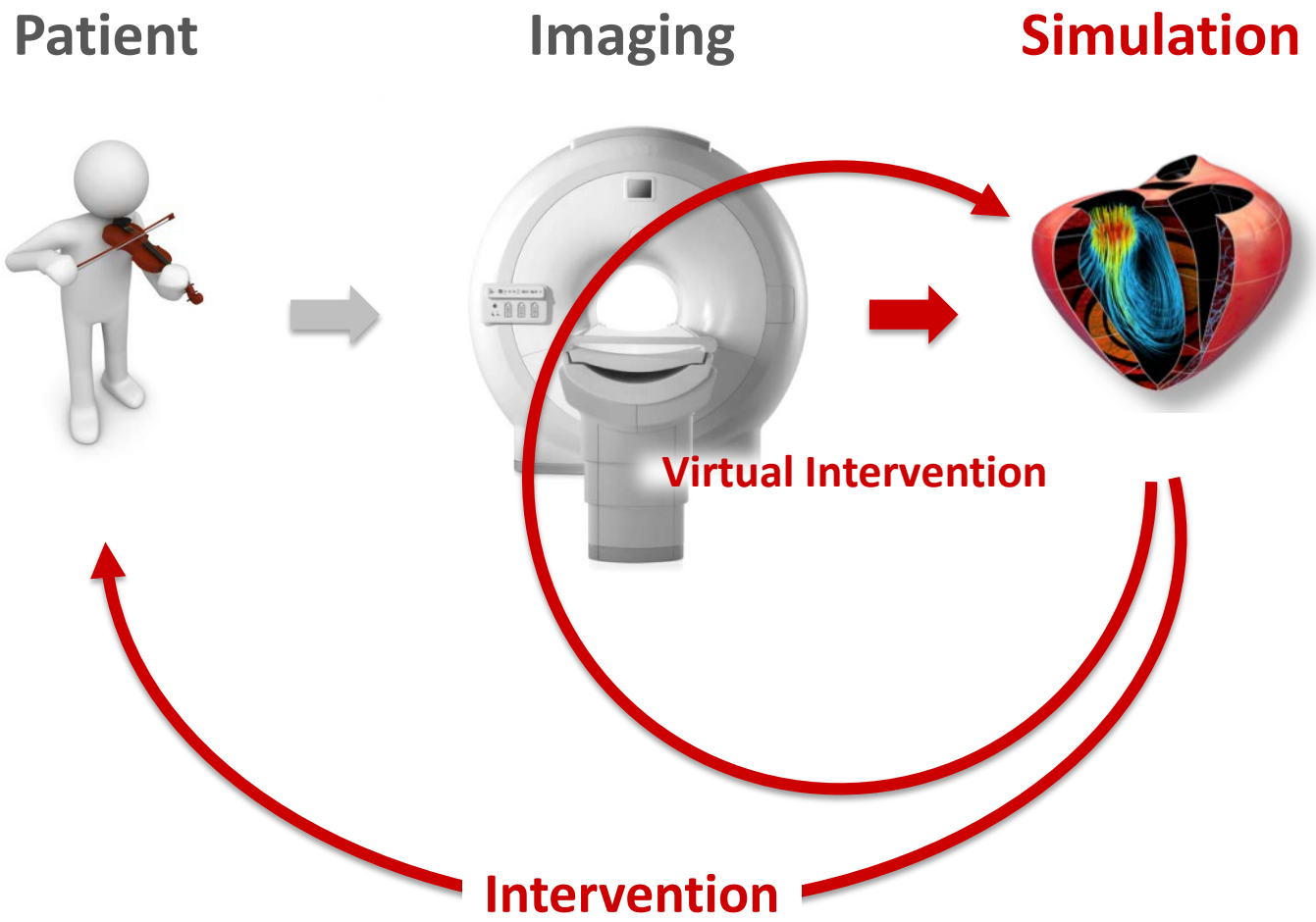

Image-guided modeling and prediction

In-vivo measurements

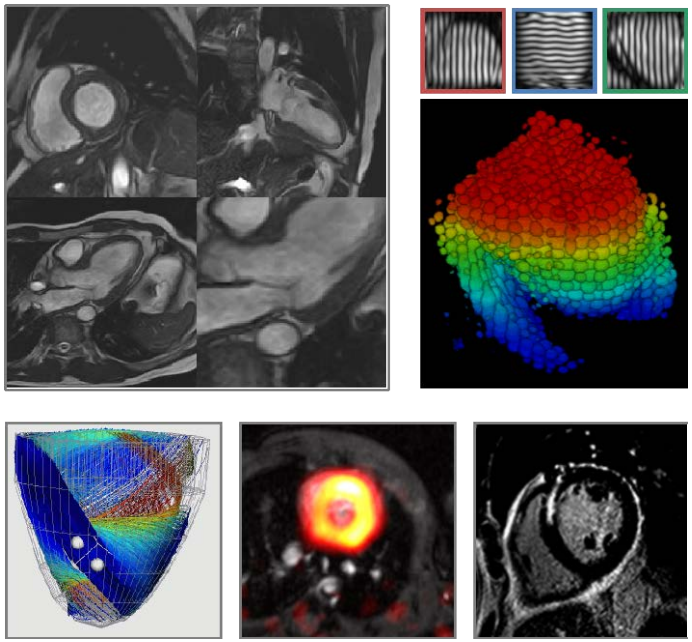

In-silico prediction

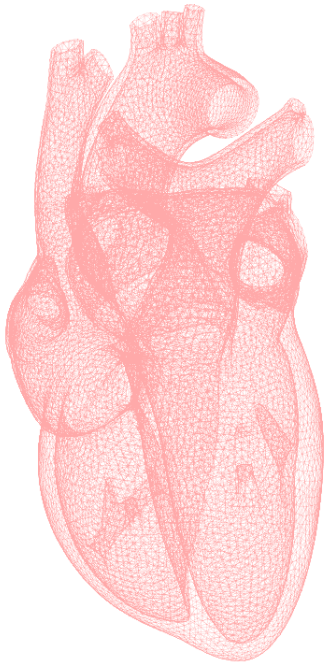

90 days

Genet M et al. J Applied Physiol 2014, J Biomech 2015

Big Data Processing

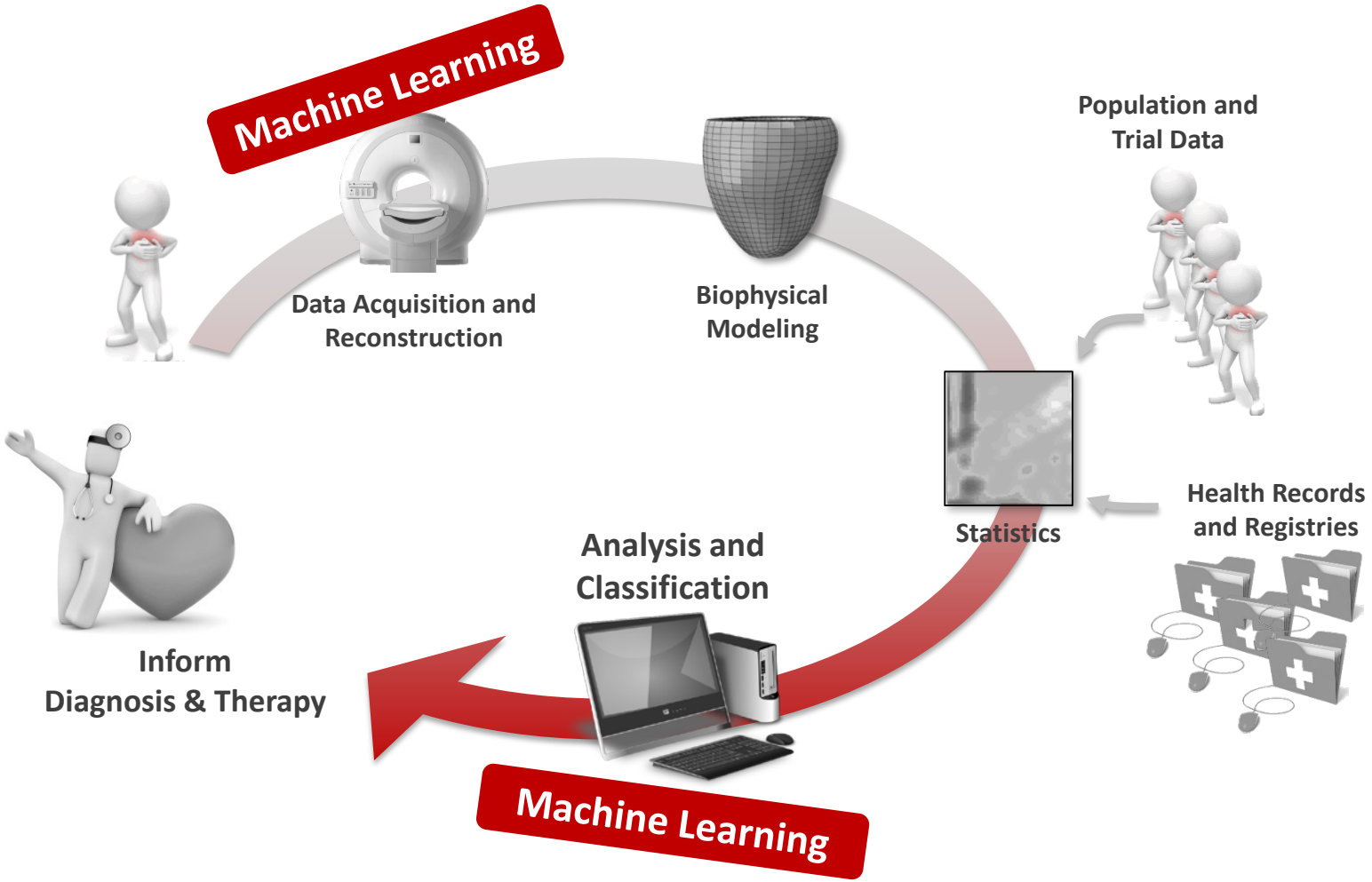

Acknowledgements

University and ETH Zurich

- Christian Stoeck
- Patrick Wespi
- Johannes Schmidt
- Verena Knobloch
- Max Fuetterer
- Julia Busch
- Lukas Wissmann
- Christian Binter
- Rudolf Fischer
- Michael Batel
- Marcin Krajewski
- Matthias Ernst
- Martin Buehrer
- Gerard Crelier
- Klaas Pruessmann

King's College London

Daniel Giese
Claudio Santelli
Constantin von Deuster
Darach O'h-ici
Nicolas Toussaint
Sven Plein

University Hospital Zurich

Robert Manka
Markus Niemann

Funding

SNF
KTI/CTI
EU FP7
EPSRC
PHILIPS